UNIVERSITY OF CALIFORNIA

SANTA CRUZ

THE CELLULAR CONSEQUENCES OF PASD1 EXPRESSION IN HUMAN CANCER

A thesis submitted in partial satisfaction
of the requirements for the degree of

MASTER OF ARTS

in

MOLECULAR, CELL, AND
DEVELOPMENTAL BIOLOGY

by

Ashley M. Kern

March 2016

The Thesis of Ashley M. Kern is
approved:

_____
Carrie Partch, Ph.D., chair

_____
Seth Rubin, Ph.D.

_____
Grant Hartzog, Ph.D.

_____
Tyrus Miller
Vice-Provost and Dean of Graduate Studies

Table of Contents

ABSTRACT

The Cellular Consequences of PASD1 Expression in Human Cancer

Ashley M. Kern

There are nearly 1,000 human proteins that are expressed only in the germline. Cancer /Testis antigens (CT antigens) represent a subset of germline-specific proteins that become reactivated in somatic cells that have undergone oncogenic transformation. Human PAS Domain containing protein 1 (PASD1) is an X-linked CT Antigen. In 2015, the Partch Laboratory established that PASD1 prevents the core circadian transcription factor, CLOCK:BMAL1, from rhythmically transcribing its target genes to suppress circadian rhythms after it becomes upregulated in cancer cells. In addition to this striking phenotype, PASD1 also promotes mitotic defects that could favor tumor progression. These phenotypes may go hand in hand; over 43% of the mammalian genome, including many cell cycle genes, is under circadian control. In this study, we found that expression of PASD1, promotes mitotic arrest, slows DNA replication, and diminishes the effects of mitotic spindle poisoning. Interestingly, preliminary data demonstrate that PASD1 is natively expressed in spermatagonia, which are testicular stem cells that undergo repeated asymmetric mitotic divisions to give rise to progenitor cells. These data support the hypothesis that expression of PASD1 in somatic cancer cells promotes premature mitotic entry, which could promote oncogenic transformation in somatic cells. The cell cycle phenotypes we observe in our study could be a consequence of reactivating the native functions of PASD1. Further studies will be required to determine if these phenotypes

are due to PASD1-mediated clock repression, or whether they arise from distinct cellular pathways regulated by PASD1 in somatic cancer cells.

Acknowledgments

Carrie Partch: You are an inspiring mentor and are a great scientist. Thanks for believing in me. You always accepted me for the person I am and I will always be grateful for your support.

Alicia Michael: This thesis would not be possible without all of your hard work on the PASD1 project. You really took me under your wing and I can't thank you enough. It was great being "lab partners" with you.

Nicolette Goularte: You are an angel and have a bright future ahead of you. Thank you so much for the crash course in Adobe Illustrator.

Partch Lab Members Past and Present: You guys rock! Thanks for always being there for me. From science to just figuring out life, you guys were the best lab mates I could have ever asked for.

Rebekah Sousae, Jessica Perez, and Bari Holm Nazario: Your guidance was appreciated. You were all a great resource to have when it came to flow cytometry topics.

Walter Bray: Thanks for running my cell lines through your group's High Throughput Cytological Screening platform. Your data was a nice contribution to my story.

Experimental Contributions

Figure 1. This schematic was adapted from Simpson et al. 2005.

Figure 2. This schematic was adapted from Cheng et al. 2011.

Figure 3. Data in panels a and b were adapted from work published by Michael et al. 2015 and Uhlen et al. 2015.

Figure 4. Data in panels a and b were adapted for this work from Michael et al., 2015. The findings reported in the table in panel c are as reported from Michael et al., 2015, Uhlen et al., 2015, and Gao et al., 2013.

Figure 5. Panels a and b were published in Michael et al., 2014 and adapted for this figure. Panel c was published in Barretina et al., 2012 and adapted for this figure.

Figure 6. The data in panels a-c were adapted from work published in Michael et al. The data in panel e were adapted from findings published in Michael et al., 2015 and an adaptation of a schematic published in Partch et al., 2014.

Figure 9. Data were collected by Walter Bray (University of California Santa Cruz Chemical Screening Center) in 2014.

INTRODUCTION

Cancer Testis Antigens

One of the oldest theories of how cancer cells arise is the "Trophoblast Theory of Cancer" proposed by John Beard over 100 years ago. In his hypothesis, Beard envisioned that cancer arose from germ cells that failed to complete their embryonic migration to the gonads (Gurchot et al., 1975). This hypothesis was quite far ahead of its time and served as the inspiration for seminal studies that examined similarities between germ cells and cancer cells. One of the first observations to support this hypothesis was the finding that many human tumors excrete the trophoblast hormone, gonadotropin (Acevedo et al., 1995). Today, the secretion of gonadotropin in somatic tissue is an established prognostic for epithelial tumor staging (Louhimo et al., 2004). Observations that establish parallels between germ cell development and tumor progression are currently on the rise and have lead to the emergence of an entire field of cancer biology, the study of Cancer/Testis antigens.

Modern studies reveal that the release of trophoblast hormones in tumors is a consequence of the aberrant expression of germline proteins in somatic tumors (Simpson et al., 2005; Whitehurst et al., 2014). In fact, many germline proteins on the X and Y chromosome are expressed in somatic human tumors. These proteins are growing in number and are known as Cancer/Testis antigens (CTAs or CT antigens). By definition, CTAs are native germline proteins that become activated and expressed in somatic cancer cells. Although most CTAs are natively expressed only in the testis,

some are also expressed in trophoblasts and immature cells of the fetal ovary (Scalan et al., 2004; Whitehurst et al., 2014; Scudellari et al., 2011; Simpson et al., 2005; Djureinovic et al., 2014; Nelson et al., 2007).

CT antigens are hypothesized to promote the activation of otherwise silenced gametogenic properties such as self renewal, pluripotency, and clonal mitotic expansion (Simpson et al., 2005). These properties are advantageous for tumors, where promotion of these properties makes it permissible for malignant populations to expand and further differentiate (Voutsadakis et al., 2015). These assertions are not surprising; oncogenic transformation and germ cell differentiation pathways share some common biological features. These features include heightened levels of cell division, the ability to induce angiogenesis, expression of chronic gonadotropin, and the downregulation of the major histocompatibility complex required for immune recognition (Figure 1). So far, over 255 CT antigens have been identified. However, the function of many CT antigens in their native context and in somatic cancer cells remains largely unknown (Whitehurst et al., 2014; Scalan et al., 2004; Simpson et al., 2005).

Efforts to find tumor proteins like CT antigens were spearheaded in the mid-1980s by a now antiquated method called autologous typing. This is a method where transformed cells are cultured *in vitro* from tumor samples and utilized as targets for immune recognition by a patient's antibodies and T cells (Old et al. 1981, Kruth

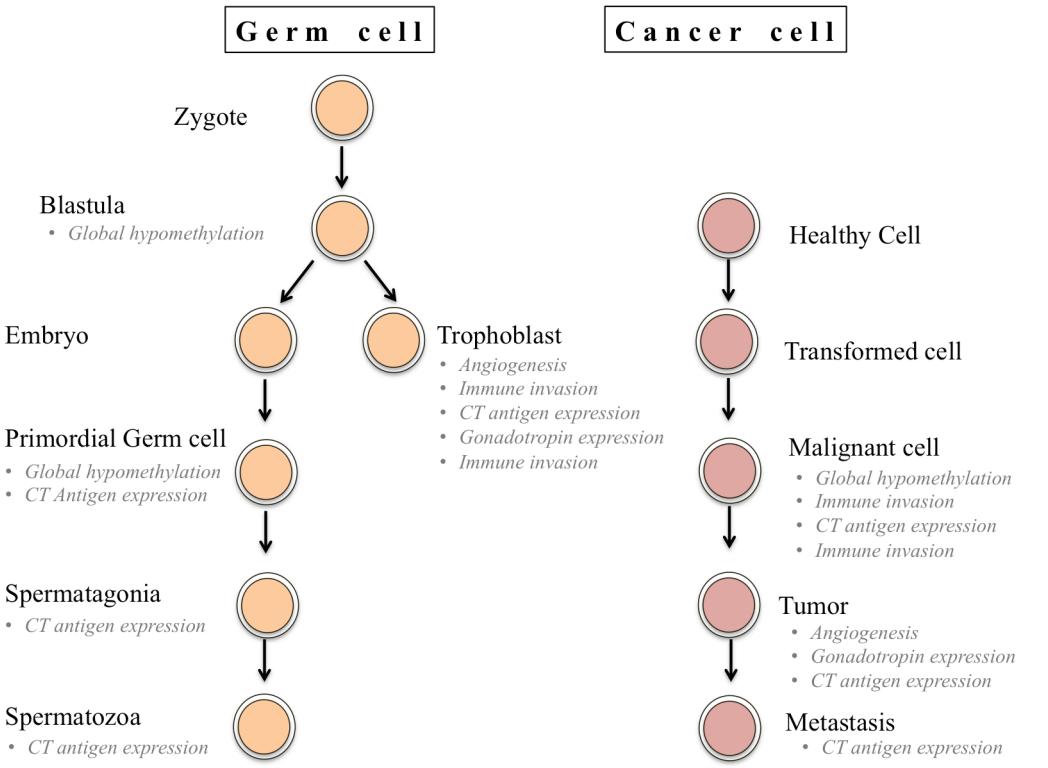

Figure 1. Cancer Testis Antigens share features of Primordial Germ Cells. Phenotypes common to both germ cells (orange) and cancer cells (red) include demethylation, induction of angiogenesis, immune invasion by the downregulation of the major histocompatibility complex, and expression of chronic gonadotropin. This figure was adapted from Simpson et al. 2005.

1984). The first CT antigen, Melanoma Antigen 1 (MAGEA1) was discovered in this fashion, and its discovery heightened interest in CT antigens as biomarkers of disease and targets for cancer vaccines. MAGEA1 is natively expressed in the testis and its expression is reported in melanoma and breast tumors. The development of autologous typing also lead to the discovery of a large number of MAGEA1 related genes that cluster on the X chromosome locus that exhibit testis restricted expression. In 1995, autologous typing was replaced by Serological Analysis of cDNA Expression Libraries (SEREX) specific to antigens of interest. By the use of this method, a large number of other somatic tumor antigens with immune reactivity, including those that are mutated or overexpressed, were identified (Old et al., 1998; Djureinovic et al., 2014; Nelson et al., 2007; Simpson et al., 2008).

Clinically, the main focus in the CT antigen field is to identify approaches that take advantage of the low, focal expression of CTAs in tumors. Initial interest in CT antigens was spurred by the search for tumor-specific immunogenic antigens that could be exploited to use the cytolytic properties of the human immune system to destroy cancer cells. CT antigens fit this bill because they are expressed with high specificity in many tumors, but absent from normal tissues. Many CT antigens are currently being considered for targets in vaccine development (Van der Brugen et al., 1991; Simpson et al., 2008). Vaccines specific to the X-linked CT antigens MAGEA1 and New York Esophageal Protein 1 (NY-ESO-1) are currently under evaluation for clinical trials in non-small cell lung cancer (Whitehurst et al., 2014). Additionally, all

published work on PASD1 prior to the discovery of its role in circadian repression has been focused on creating cancer vaccines specific to PASD1 (Ait-Tahar et al., 2009; Cooper et al., 2006; Joseph-Pietras et al., 2010; Liggins et al., 2004; Sahota et al., 2006; Michael et al., 2015).

Pinning down specific roles for CT antigens in gametes would provide insight into the consequences of the reactivation of CT antigen expression on cancer progression and outcomes. Many CT antigens are expressed throughout spermatogenesis (Simpson et al. 2005; Whitehurst et al. 2013, Scalan et al. 2002) (Figure 2). For example, MAGEA1 and NY-ESO-1 are expressed during early spermatogenesis (Simpson et al., 2005; Whitehurst et al., 2013). Other interesting CT antigens implicated in spermatogenesis include Cytochrome C Oxidase subunit II (COXB2) and Spermatogenesis Protein 19 (SPATA19). COXB2 is a complement of complex IV of the electron transport chain and SPATA19 was identified as a mitochondrial adhesion protein required for sperm motility (Cheng et al. 2011; Whitehurst 2014). Many CT antigens are not just expressed during spermatogenesis, but are also essential for fertility. In mice, homozygous and heterozygous deletions of ADAM Metallopeptidase Domain 2 (ADAM2) or ADAM Metallopeptidase Domain 3 (ADAM3) lead to normal development but complete loss of fertility (Han et al., 2010). Taken together, CTAs appear to be important for germline development and function, but are clearly not essential in somatic tissues.

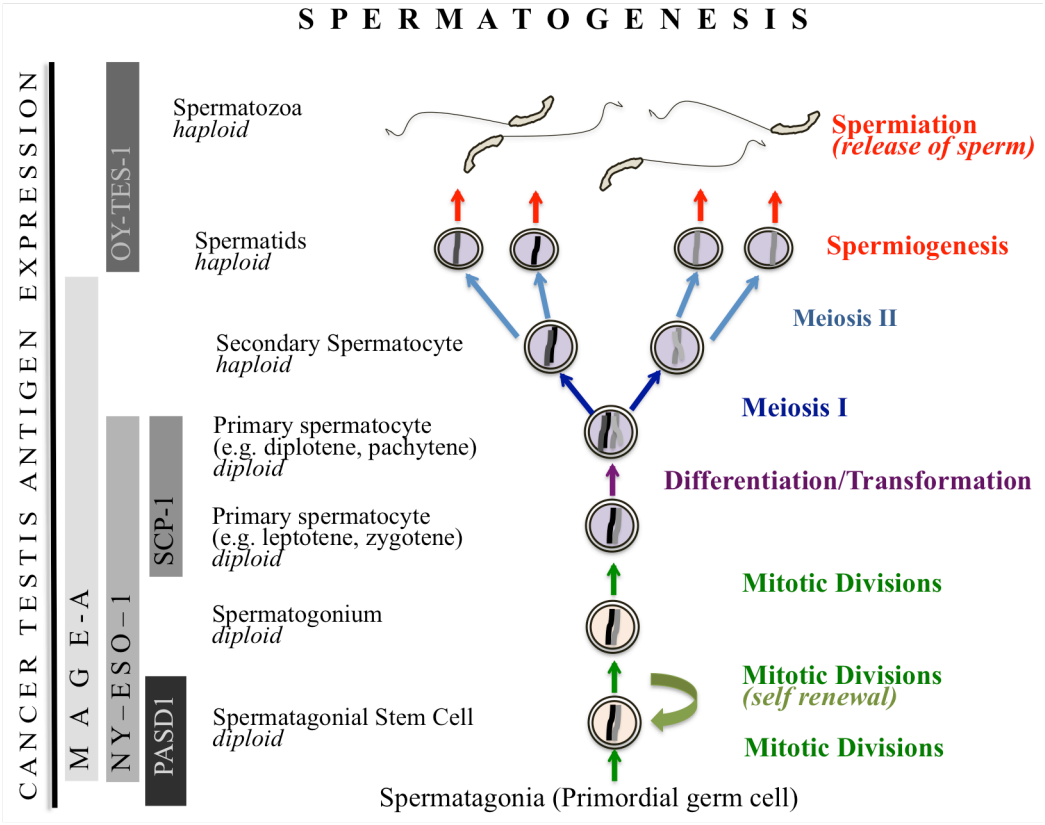

Figure 2. Cancer Testis Antigens and PASD1 are Expressed Throughout Spermatogenesis

Depicted is a schematic showing the temporal expression pattern of select CT antigens in germ cells during spermatogenesis. Labeled on the right is the progression of germ cell types throughout spermatogenesis, and on the left, are the expression patterns of five different CT antigens in various germ cell types. This figure was adapted from Cheng et al. 2011

The Expression of Cancer Testis Antigens in the Soma Promotes Oncogenic Transformation

The expression of CT antigens is found in many human somatic cancers (Whitehurst et al., 2014; Simpson et al, 2015; Uhlen et al., 2015, Gao et al., 2013) (Figure 4)(Figure 5). For example, recent work has identified over twenty CT antigens as overexpressed in non-small cell lung cancer (Scalan et al., 2004; Sugita et al., 2002). In healthy somatic cells, CT antigen gene promoters exist in a hypermethylated, inactive state that prevents their expression (Simpson et al., 2005). Conversely, demethylation of these loci is used to activate CT antigens in the germline during gametogenesis and early embryogenesis. It is hypothesized that many CT antigens use demethylation to become reactivated in somatic cancer cells. Upon reactivation in the soma, transformed cells are proposed to take on features of primordial germ cells like self-renewal, uncontrolled proliferation, and the ability to complete an epithelial-to-mesenchyme transition (Simpson et al., 2005; Abell et al., 2010; Ugarte et al. 2015). Ultimately, tumor-specific epigenetic alterations of CTAs are thought to promote otherwise silenced genetic programs that could be exploited to promote neoplastic phenotypes.

Classically, the activation of CT antigen genes in somatic cancer cells was thought to occur only through the demethylation of CpG islands within gene promoter regions (Webber et al., 1994). This was first demonstrated by in experiment where Weber et

al. showed that treatment with the DNA hypomethylating agent, 5-aza-2′-deoxycytidine (5-AZA-CdR) activated *de novo* expression of the MAGEA1 gene in a human melanoma cell line (Weber et al., 1994). Later, it was shown that the MAGEA1 gene expression correlated with the methylation status of its promoter in neoplastic cells of varied histologies (De Smet et al., 1996). This was also shown to be true in many different MAGE related genes such as NY-ESO-1 where their expression was found to be associated with the hypomethylated status of their promoters in tumors and human cancer cell lines (De Smet et al., 1996; De Smet et al., 2004; Honda et al., 2004). However, recent studies suggest that demethylation of CpG islands within gene promoter regions is not the only way that CT antigens can become activated. In a systematic analysis of DNA methylation profiling data from various tissue types by Kim et al., it was also found that the hypomethylation of CT antigens clusters into nuclear associated domains throughout the genome that coincide with nuclear lamina-associated domains. It was also observed in this study that there is no significant difference in the hypomethylation pattern between CTAs without CpG islands and CT antigens with CpG islands in the proximal promoter (Kim et al., 2013)

There is clinical evidence to support the hypothesis that CT-X antigen activation in the soma is primarily mediated by alternations in DNA methylation. For example, it was found that there is significant demethylation of the MAGEA1 promoter in non-small cell lung cancer tumor samples of individuals with a history of smoking (Jang

et al., 2001). Additionally, exposure to demethylating agents were sufficient to activate numerous CTAs in the soma, suggesting that this may be a conserved mechanism of reactivation (Loriot et al., 2006; James et al., 2006). Furthermore, mechanisms aside from methylation may also contribute to CT antigen reactivation, as inhibition of histone deacetylases has also been shown to reactivate CTAs in somatic cancer cells (Simpson et al., 2005). Ultimately, the epigenetically tractable nature of CT antigens appears to provide a platform that is particularly sensitive to reactivation in tumors, where misregulation of methylation programs is quite common (Brait and Sidransky, 2012; De Smet et al., 1996).

Some CTAs are implicated in the promotion of tumor progression by facilitating cancer cell survival or enhancing the overactive signaling of oncogenes. One example is ATPase Family AAA domain Containing 2 (ATAD2). ATAD2 helps facilitate cell survival in Retinoblastoma-associated (RB) protein-deficient tumors. In this tumor type, ATAD2 can become activated by E2F Transcription Factor 1 (E2F1) to act a co-factor for c-myc-mediated transcription. High levels of ATAD2 are correlated with poor survival in breast cancer patients (Ciro et al., 2009; Kalashnikova et al., 2010), whereas deletion of ATAD2 reduces cell proliferation and S-phase entry. In a second example, the expression of the MAGE gene family has classically been correlated with tumorgenesis. MAGE proteins enhance ubiquitin ligase activity by directly binding E3 ligases (Pineda et al., 2015; Pineda and Potts, 2015). In 2010, the CT

antigen MAGEC2 was found to interact with Tripartite Motif (TRIM) family proteins and increase degradation of Tumor Protein 53 (TP53, or p53) in p53-expressing tumor cells (Doyle et al., 2010).

One of the most notable players in the pathology of cancer is aberrant mitotic progression caused by defective mitotic machinery (Geert et al., 2005). One example of a CT antigen that promotes this phenotype is Testis Expressed Gene 14 (TEX14). When TEX14 is expressed in somatic cells, it delays mitotic exit. TEX14 is expressed natively in the testis in early spermatogenesis, where it helps to sequester Centrosomal Protein of 55 kDa (CEP55) and prevent premature cell abscission at the midbody during cytokinesis (Mondal et al., 2010; Bastos et al., 2010). These data go hand in hand with the theme of this work, where the expression of a CTA in somatic cancer cells promotes mitotic defects.

Therefore, there is a strong body of evidence to suggest that reactivation of select spermatogenesis-associated CT antigens may influence mitotic fidelity in cancer cells. In 2010, the Whitehurst group found that the CT antigen, Acrosin Binding Protein (ACRBP) interacts with the Nuclear Mitotic Apparatus Protein 1 (NUMA1), a key component of the mitotic spindle when it is expressed in cancer cells. As a result of this interaction, ACRBP restricts NUMA1 dependent abrogation of mitotic spindle assembly. They found that this phenotype was also instrumental in reinforcing the fidelity of mitotic spindles when cancer cells are treated with the microtubule

poisoning chemotherapeutic Paclitaxel (Whitehurst et al., 2010). In 2012, the Whitehurst group used a genome-wide small interfering RNA (siRNA) screen to demonstrate that CT antigens could confer resistance the mitotic spindle poisoning chemotherapeutic, Paclitaxel. In their screen, they knocked down the expression of CT antigens or testis-biased proteins and their knock down of target genes resulted in Paclitaxel sensitivity. In this screen they also asked if these hits also had defects in chromosome segregation, bipolar spindle formation, or interphase microtubule dynamics using microscopy. They identified a role for five testis-specific proteins in the promotion of mitotic entry in non-small cell lung cancer. Not surprisingly, one of these was a MAGE family protein, MAGEA5. Ultimately, these studies support the notion that the reactivation of testis-restricted gene products in somatic cancer cells may reinforce the integrity of the mitotic spindle and diminish the impacts of mitotic spindle-targeting chemotherapeutics.

PASD1 is a Clinically Relevant Cancer Testis Antigen

Natively, PASD1 is expressed exclusively in the human germline and shows the highest expression level in cells along the basement membrane of the testis that are consistent with spermatogonial stem cells (Uhlen et al., 2015)(Figure 3). However,

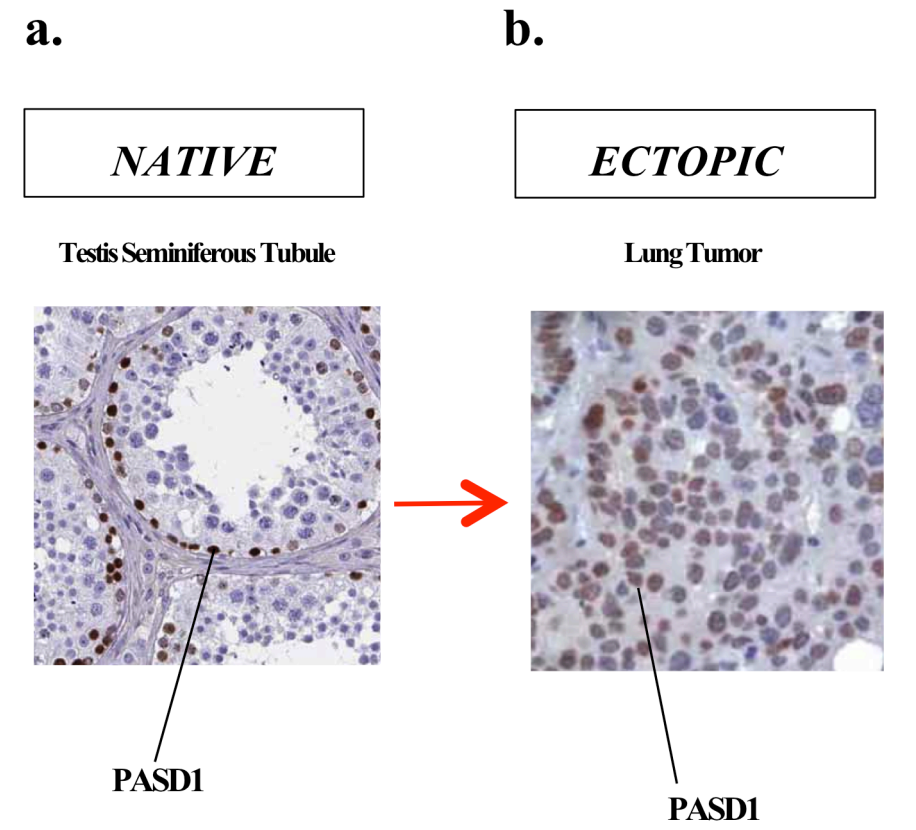

Figure 3. PASD1 is expressed in the Germline and Somatic Human Cancer Immunohistochemical staining of tissue where PASD1 expression is detected using immunoreactivity to an antibody specific to full-length PASD1 and tissue is co-stained with a hemotoxylin nuclei stain. a.) A cross section of a human testis seminiferous tubule. PASD1 expression is detected in the nuclei of cells found in the basal component of the epithelium (Uhlen et al, 2013). b.) A cross section of a human lung cancer tumor sample that contains cells that express nuclear PASD1.

after oncogenic transformation, PASD1 becomes expressed in a large array of human somatic cancers and cancer cell lines (Ait-Tahar et al., 2009; Cooper et al., 2006; Liggins et al., 2004; Michael et al 2015; Uhlen et al., 2015, Gao et al., 2013). These findings are also supported by a recent RNAseq study done by the National Institutes of Health TCGA Cancer Genome Atlas Consortium where PASD1 mRNA was found only in the testis of healthy individuals, but in a diverse array of human cancer histologies (Gao et al., 2013) (Figure 4). Although the expression of PASD1 is not exceedingly high in tumor samples, it is expressed in somatic tissues where it should be transcriptionally silent. (Gao et al., 2013; Sahota et al., 2006; Cooper et al., 2006; Liggins et al., 2010; Michael et al., 2015) (Figure 4).

Interest in studying PASD1 expression in human cancer came from the finding that PASD1 is expressed in multiple melanomas at transcript levels at a frequency greater than what is reported for NY-ESO-1, a classic CT antigen and therapeutic target (Sahota et al., 2006). Like many cancer testis antigens of clinical interest, expression of PASD1 can induce a cytolytic T cell immune response in humans (Cooper et al., 2006; Liggins et al. 2006; Pietras et al., 2010). Moreover, patients with peripheral T-cell lymphoma produced circulating antibodies capable of recognizing PASD1 (Liggins et al., 2006). These findings were instrumental in the development of cancer vaccines designed to target PASD1, including one specific to full-length PASD1 that induced cytotoxic T lymphocytes capable of lysing human multiple melanoma with endogenous PASD1 expression (Pietras et al, 2010).

a.

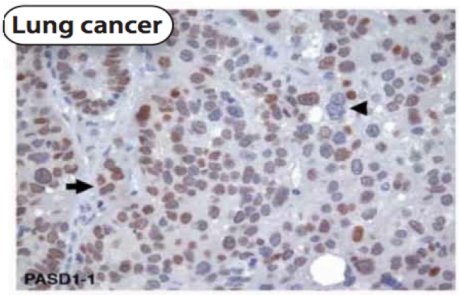

b.

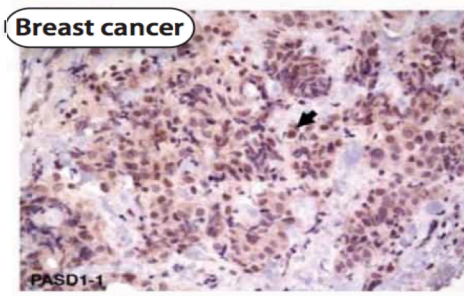

c.

Disease Site	Histology	Study
Brain	Glioblastoma muliforme Adrenocortical Carcinoma Pheochromocytoma Low Grade Glioma	Gao et al., 2013, Uhlen et al., 2015
Head & Kneck	Squamous Cell Carcinoma	Gao et al., 2013, Uhlen et al. 2015
Thyroid	Thyroid Carcinoma	Gao et al., 2013, Uhlen et al. 2015
Skin	Uveal Melanoma Cutaneous Melanoma	Gao et al., 2013, Uhlen et al. 2015
Connective Tissue	Sarcoma	Gao et al., 2013
Blood	Acute Myeloid Leukemia Large B-Cell Lymphoma	Gao et al., 2013
Lung	Non-small cell carcinoma	Gao et al., 2013,Micheal and Anderson, 2014, Unpublished, Uhlen et al. 2015
	Adenocarcinoma Squamous Cell Carcinoma	Gao et al., 2013
Breast	Epithelial Cell Carcinoma	Micheal and Anderson, 2014, Unpublished., Uhlen et al. 2015
	Invasive Carcinoma Mesothelioma	Gao et al., 2013
Stomach	Adenocarcinoma	Gao et al., 2013, Uhlen et al. 2015
Bile Duct	Cholangiocarcinoma.	Gao et al., 2013
Pancreus	Adenocarcinoma	Gao et al., 2013, Uhlen et al. 2015
Liver	Heptocarcinoma	Uhlen et al. ,2015
Kidney	Paillary Cell Carcinoma	Gao et al., 2013, Uhlen et al. 2015
	Clear Cell Carcinoma Chromophobe	Gao et al., 2013
Ovary	Serous Cystadeocarcinoma	Gao et al., 2013, Uhlen et al. 2015
Uterine	Corpus Endometrioid	Gao et al., 2013, Uhlen et al. 2015
	Carcinosarcoma	Gao et al., 2013
Cervix	Endocervical Carcinoma	Gao et al., 2013
Prostate	Adenocarcinoma	Gao et al., 2013, Uhlen et al. 2015
Testis	Germ Cell Carcinoma	Gao et al., 2013, Uhlen at al. 2015, Uhlen et al. 2015
Colon	Adenocarcinoma	Gao et al., 2013, Uhlen at al. 2015

Figure 4. PASD1 is Expressed in Many Somatic Human Cancer Histologies
Immunohistochemical staining of tissue where PASD1 expression is detected using immunoreactivity to an antibody specific to full-length PASD1 and in fixed tissue that is co-stained with a hemotoxylin nuclei stain. The arrows indicate examples of cells that express PASD1. a.) A cross section of a human lung cancer tumor. b.) A cross section of a human breast cancer tumor that contains cells that express nuclear PASD1. c.) Table detailing the expression of PASD1 in somatic human cancer as determined by immunohistochemistry and mRNA expression profiling of human tumors (Michael et al., 2014; Uhlen et al. 2015; Gao et al., 2013).

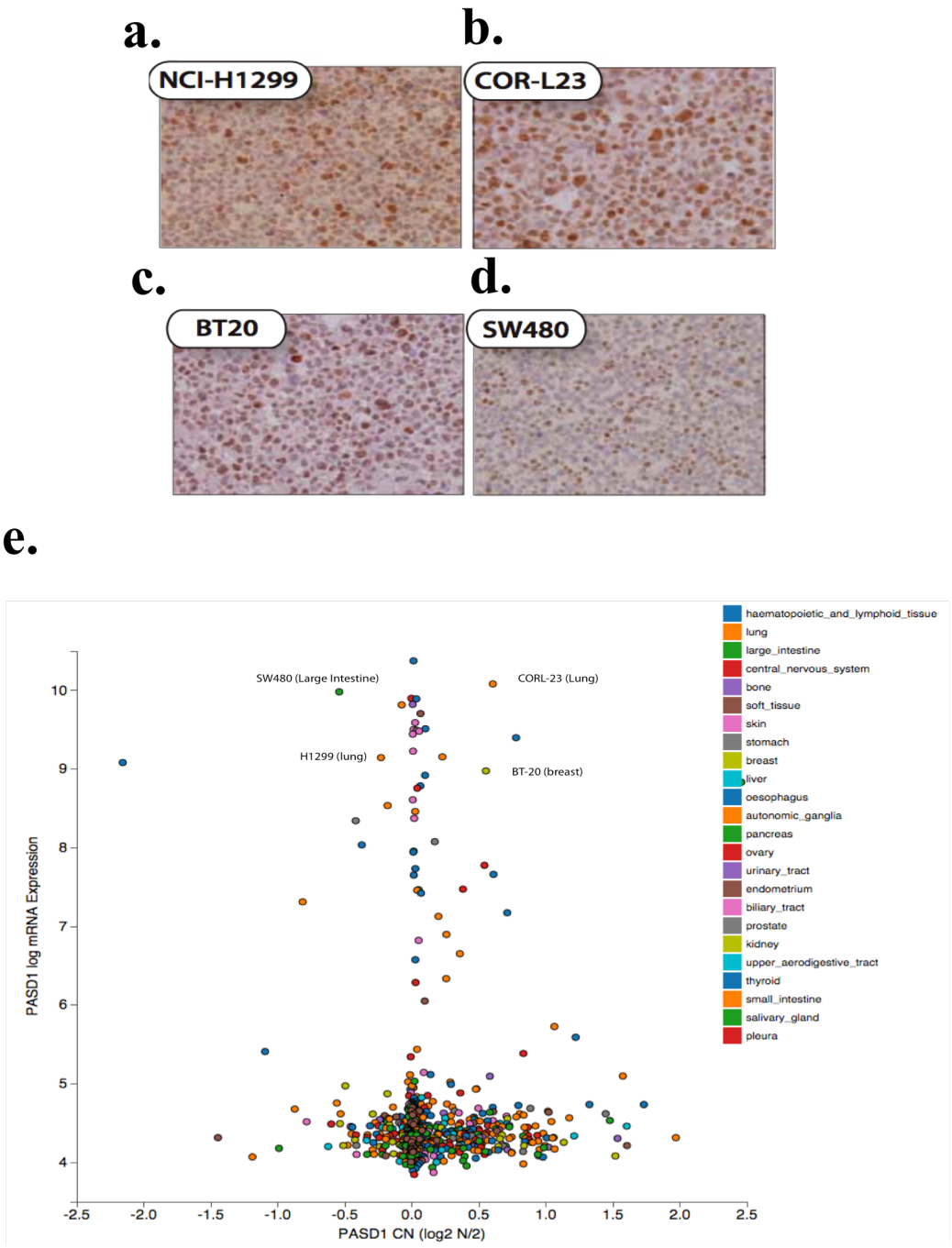

Figure 5. PASD1 is expressed in Human Cancer Cell Lines
Immunohistochemical staining of human cell lines that express PASD1 detected by immunoreactivity to an antibody specific to full-length PASD1. a.) H1299, a non-small cell lung cancer cell line b.) CORL-23, a large cell carcinoma lung cancer cell line. c.) BT-20, a breast cancer cell line d.) SW480, a colorectal cancer cell line. e.) Volcano plot depicting PASD1 transcript copy number vs. log-fold mRNA expression as measured by RNAseq analysis of various human cancer cell lines collected by Barretina et al., 2012.

Evaluating the Cellular Consequences of PASD1 expression in Somatic Cells

One of the most striking characteristics of PASD1 that it is an X-linked gene that is broadly conserved in mammals, with the exception of the murine lineage. This unusual lineage restriction of PASD1 expression is a property unique to X-linked genes involved in human spermatogenesis (Mueller et al., 2013). The expression pattern of PASD1 in the testis suggests that PASD1 could be involved in spermatogenesis and is expressed in spermatagonia (Uhlen et al., 2015)(Figure 3). However, it remains to be shown that PASD1 co-localizes with stem cell markers. These data are quite intriguing because spermatagonia are stem cells that eventually give rise to haploid spermatozoa (Cheng et al., 2011).

Spermatogenesis is a highly coordinated process that begins with the clonal expansion of spermatagonia in the basement membrane of the seminiferous tubules of the testis (Cheng et al., 2011). There are two subtypes of spermatagonia; Type A and Type B. Type A Spermatagonia act as progenitor cells that undergo multiple rounds of mitosis and asymmetric cell division. In this process, one daughter cell under goes another round of mitosis to renew the Type A stem cell pool, and then the other differentiates into Type B Spermatagonia, which migrate into the lumen of the seminiferous tubules. Here, they differentiate into spermatocytes and enter meiosis. Meiosis results in haploid spermatozoa that differentiate into sperm (Rato et al., 2012) (Figure 2). These data resonate with our findings, where we report that PASD1 induces mitotic defects and appears to PASD1 natively in spermatagonia. Take

together, these data argue that one potential consequence of PASD1 reactivation in somatic cancer cells could be promotion of mitotic entry.

The human testes are an immune-privileged environment. Together, the blood-testis-barrier (BTB) and the Sertoli cells of the basal epithelium of the seminiferous tubules work to protect testis proteins from attack by the immune system. To do this, the BTB acts as a physical barrier and Sertoli cells secrete humeral factors such as interleukins, interferons, and cytokines to contribute to immune protection (Cheng et al., 2011). Meiosis I and II, and spermatogenesis take place in the apical compartment of the seminiferous epithelium, while spermatagonia renewal, differentiation, and mitosis occur in the basal compartment of the epithelium (Cheng et al., 2012). This biology, and the fact that PASD1 is expressed in the basal epithelium near Sertoli cells argues for the possibility that PASD1 may respond or potentiate cytokine signaling. In fact, expression of PASD1 in cancer cells was recently found to activate the release of IL-6 ligand, an important cytokine implicated in immune protection (Xu et al., 2016; Heinrich et al., 2003). These data suggest that PASD1 could help somatic cancer cells evade immune detection by secreting protective cytokines.

The overexpression of other cellular components, like cell signaling molecules, is implicated in many human cancers (Santarius et al., 2010). For example, the overexpression of Epidermal Growth Factor (EGFR) is biomarker for head and neck, ovarian, cervical, bladder, and esophageal cancer. In these cancers, an increase in

EGFR expression is positively correlated with reduced recurrence-free survival (Nicholson et al., 2001). Like EGFR, the activation of the proto-oncogene, Signal Transducer and Activator of Transcription 3 (STAT3) promotes tumor growth by enhancing the expression of genes required for cell survival/proliferation, motility and immune tolerance (Avalle et al., 2012).

PASD1 potentiates Janus Kinase (JAK) / STAT3 signaling pathways in human cancer cells (Xu et al. 2016). In their study, Xu et al. found that the overexpression of PASD1 activates STAT3 nuclear release and the transcription of downstream target genes. They determined that PASD1 mediates this through two different mechanisms; through IL-6 ligand stimulation and also through direct interaction with STAT3. The IL-6 ligand is a highly pleiotropic cytokine that has roles in signal transduction, the immune response, inflammation, and hematopoiesis (Heinrich et al., 2003). In signal transduction, Il-6 ligand stimulates the trans-phosphorylation and activation of IL-6 receptor-bound Janus kinase (JAK). Upon activation, JAK phosphorylates and activates STAT3, permitting its release and translocation to the nucleus (Nishimoto and Norihiro, 2006). PASD1 interacts directly with STAT3 and competes the nuclear tyrosine phosphatase TC45 to prevent STAT3 inhibition (Xu et al. 2016). The significance of these findings was also demonstrated *in vivo*, where the knockdown of PASD1 inhibited the expression of proto-oncogenes, which suppressed anchorage-independent growth, cell migration, and inhibited tumor growth in a xenograph

mouse model (Xu et al., 2016). Like many CT antigens, the expression of PASD1 in somatic cancer cells could promote tumor progression.

PASD1 Impairs the Molecular Circadian Clock When Expressed in Human Cancer Cells

Given the widespread expression of PASD1 in somatic cancers, it is important to further understand other consequences of PASD1 expression in somatic cancer (Michael et al., 2015; Uhlen et al. 2015; Sahota et al., 2006)(Figure 3 and 4). In 2015, our lab established that PASD1 is a repressor of the core circadian clock transcription factor, CLOCK:BMAL1, and suppresses circadian rhythms in human cancer cells (Michael et al. 2015)(Figure 6b,d). Any disruption of the clock through environmental stimuli or genetic means can to lead to the onset of diseases such as diabetes, cancer, and cardiovascular disease (Partch et al. 2014; Jeyaraj et al., 2012; Kondratov et al., 2006; Marcheva et al., 2010).

The molecular clock is cell autonomous and driven by two interlocked transcription/feedback loops. CLOCK:BMAL1 sits at the core of the molecular circadian clock in mammals and is a heterodimeric basic helix-loop-helix (bHLH)-PAS transcription factor (Figure 6d). In the core transcriptional feedback loop, CLOCK:BMAL1 sits at the positive where it transcribes its own repressors, *Period* and *Cryptochrome,* and other clock-controlled genes. PER and CRY proteins drive the negative arm of the feedback loop, where they form a complex and translocate to

the nucleus to directly interact with CLOCK:BMAL1 to inhibit transcriptional activation. A second feedback loop is interlocked with this core oscillator because CLOCK:BMAL1 drives the expression of the Retinoid Retinoid-Related Orphan Receptor family (RORa, RORb, and RORc) (Sato et al., 2004). Like CLOCK:BMAL1, these receptors drive the transcription of their own repressors, REV-ERBα and REV-ERBβ (Preitner et al., 2002). This secondary loop ensures the rhythmic transcription of *Bmal1* (Ukai-Tadenuma et al, 2011). Together, these interlocked feedback loops control expression of 43% of the genome on a daily basis to confer temporal regulation to biological processes (Zhang et al., 2014).

Our lab's initial interest in PASD1 came from our observation that there is a significant conservation between PASD1 and CLOCK. These regions include the PAS-A domain and a coiled-coil region in PASD1 (CC1) that is similar to exon 19 of CLOCK, both of which are required for CLOCK:BMAL1 function (Gekakis et al., 1998; Katada and Sassone-Corsi, 2010; King et al., 1997; Michael et al., 2015;) (Figure 6a). PASD1 diverges from the domain organization of CLOCK in that it lacks domains critical for transcriptional activation, such as the DNA binding basic Helix-Loop-Helix domain (bHLH) (Huang et al., 2012) (Figure 6a). Mutagenesis studies of PASD1 reveal that the CC1 region of PASD1 is required for repression. PASD1 is hypothesized to repress the transcription of clock-controlled genes through interactions with the CLOCK:BMAL1 complex. This model is proposed because PASD1 and CLOCK:BMAL1 were found to co-immunoprecipitate, suggesting that

they interact (Michael et al. 2015). The discovery of a cancer-induced repressor of the circadian clock is significant because the clock coordinates temporal control of roughly 43% of the mammalian genome (Zhang et al., 2014). Although the molecular circadian clock is well characterized as a global transcriptional regulator, the identification of additional factors that could provide tissue-specific regulation of clock outputs remains largely unknown (Partch et al., 2014).

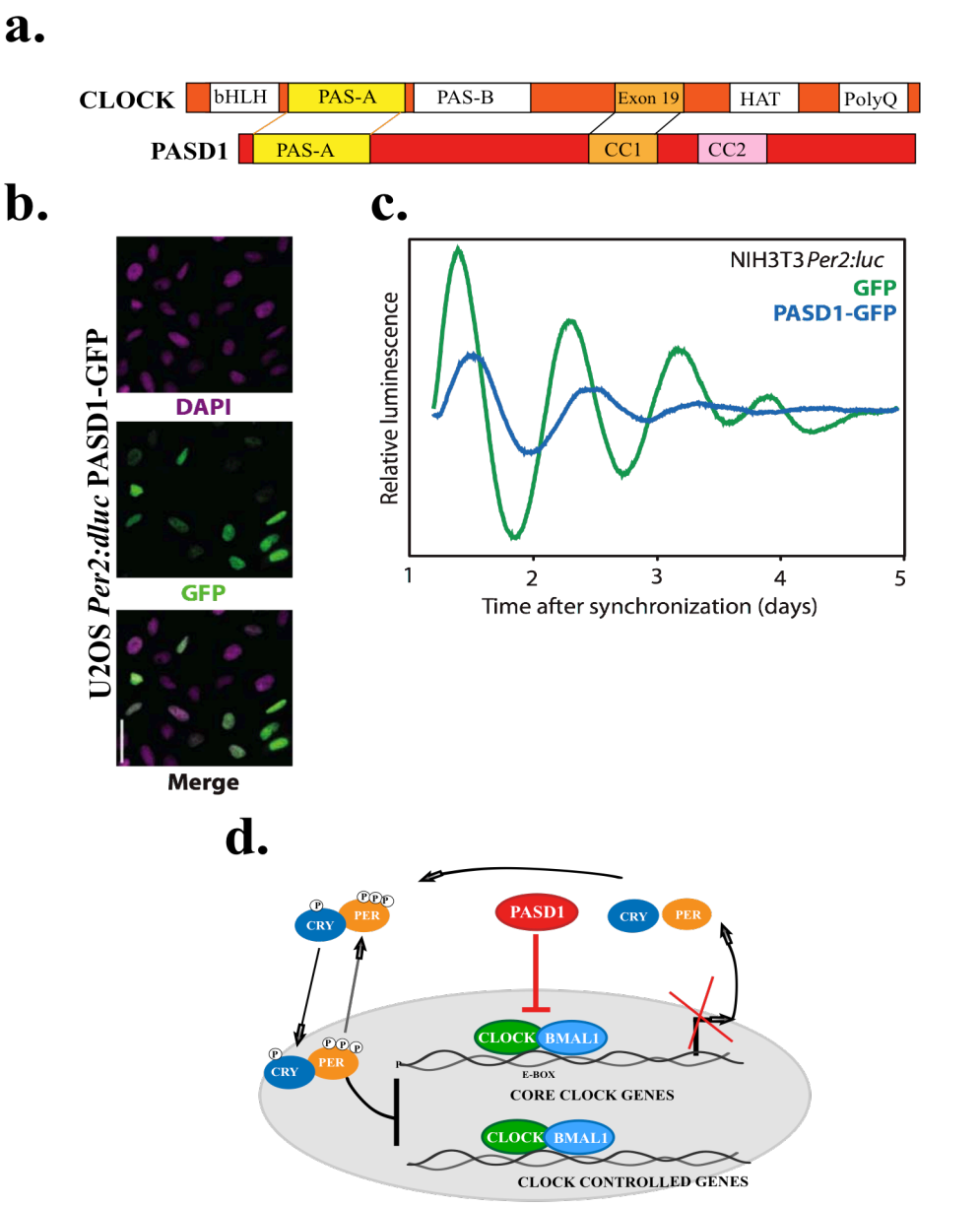

Figure 6. PASD1 is a Nuclear Protein With Homology to CLOCK that Represses the Activity of the Circadian Clock

a.) PASD1 has significant homology to the circadian transcription factor CLOCK, with conservation between the PAS-A domains and the Exon 19 region of CLOCK. b.) PASD1-GFP is exclusively nuclear when expressed in a U2OS human osteosarcoma cancer cell line and co-localizes with nuclear staining (DAPI) in the nucleus. c.) Expression of PASD1-GFP dampens the period and amplitude of *Per2* gene expression as measured by luciferase bioluminescence in mouse NIH3T3 *Per2:dluc* fibroblasts. d.) Working model: PASD1 inhibits the ability of CLOCK:BMAL1 to transcribe its target genes by inhibiting the transcriptional activity of CLOCK:BMAL1 through interactions with the complex.

Summary

Here, we present work where we employ a cell biology approach to examine the consequences of PASD1 expression in somatic cancer cells. Although the native function of PASD1 in the germline remains to be studied, PASD1 has an expression pattern that suggests it may be natively localized to the nuclei of spermatagonial stem cells. The expression pattern of PASD1 allows us to infer that it may regulate renewal and/or mitotic divisions in spermatagonia in the seminiferous tubules (Cheng et al, 2011; Rato et al., 2012). Thus, if PASD1 is ectopically expressed in somatic cancer cells, it seems plausible to predict that PASD1 could promote aberrant mitotic entry or enhance the function of proteins involved in assembling the mitotic spindle. These assertions are in line with the finding that many Cancer Testis antigens promote premature mitotic entry by impaired mitotic machinery (Cappell et al., 2012). If PASD1 were to promote mitotic defects, it would be highly significant because impaired mitotic machinery and a loss of control of mitotic timing can promote aneuploidy and resistance to chemotherapy drugs (Hassold et al., 2001; Whitehurst et al., 2007).. Ultimately, we aim to further characterize potential PASD1 mediated mitotic defects in human cancer cells.

RESULTS

PASD1 Induces G2/M Arrest

The native expression pattern of PASD1 and the established literature on CT antigens made us curious about the effects of PASD1 on mitotic entry. To study the effects of

PASD1 expression on circadian gene oscillation and other cellular phenotypes, we first created a U2OS cell line with the *Per2:dluc* reporter (Michael et al. 2015). In the circadian biology field, a common method to circadian gene cycling is to express a rapidly degradable form of luciferase, *dLuc*, driven by the mouse *Per2* gene promoter (*Per2:dluc*) to monitor circadian gene oscillation *in vitro* (Liu et al., 2008). Next, we created another cell line that constitutively expresses PASD1 fused with C-terminal GFP (PASD1-GFP) under control of the cytomegalovirus (CMV) promoter in our previously established U2OS *Per2:dluc* cells. As a control for the consequences of overexpressing GFP, we also created a U2OS *Per2:dluc* GFP line (Michael et al. 2015). After establishing our U2OS cell line, in culture, we noticed that U2OS *Per2:dluc* PASD1-GFP cells took longer to reach confluency than their GFP counterparts. These observations lead us to hypothesize that PASD1-GFP expression may induce abnormal cell cycle progression.

To test our hypothesis, we first asked if cells expressing PASD1-GFP had abnormal cell cycle profiles. To do this, we first transiently overexpressed full-length PASD1-GFP in a mouse fibroblast line containing the *Per2:dluc* reporter (NIH3T3). We also controlled for GFP expression by using the same construct to overexpress GFP in *Per2:dluc* NIH3T3 cells. Although the cells were not human, they offered a good platform to study the effects of PASD1 in a non-cancerous genetic background. To measure the cell cycle profiles, we used fluorescence-assisted cell sorting (FACS) to assess the DNA content in fixed cells stained with propidium iodide, a fluorescent

DNA intercalating dye. We found that PASD1-GFP expression induced a pronounced increase (17%) in the number of cells that accumulated at the G2/M phase transition when compared to control GFP cells (Figure 7a).

We then looked to recapitulate these findings in human cells using the embryonic kidney HEK-293T cell line. We transiently transfected full-length PASD1-GFP and monitored cell cycle profiles when peak expression of PASD1-GFP was reached at 48 hours. We observed that transient PASD1-GFP overexpression also induced a significant G2/M arrest here as well, where 24% more cells accumulated compared to their control GFP counterparts (Figure 7b). Next, we investigated whether this phenotype was observable in human cancer cells with exogenous overexpression of PASD1-GFP or the GFP control. To do this, we performed propidium iodide staining and FACS analysis in U2OS *Per2:dluc* PASD1-GFP and GFP cells, as well as the lung cancer cell line (H1299) and colorectal cell line (SW480), both of which contained the circadian reporter gene, *Per2:dluc*. These cells were a good panel to study the effects of PASD1 overexpression, because U2OS cells do not express PASD1, whereas H1299 and SW480 cells express PASD1 at moderate levels (Michael et al., 2015).

First, we performed the cell cycle profile assay in U2OS *Per2:dluc* cells. As observed in NIH3T3 and HEK-293T cells, PASD1-GFP expression induced a significant (12% ± 8 %) increase in the number of cells that accumulate at the G2/M transition (Figure

7c). Next we tested the other cancer cell lines that express endogenous PASD1 at moderate levels. We started by assaying our line with the highest endogenous PASD1 expression, SW480 *Per2:dluc* and found a 15% increase in the number of cells at the G2/M transition in PASD1-GFP cells as compared to GFP controls (Figure 7d).

Lastly, we subjected our H1299 *Per2:dluc* cells to our cell cycle profile analysis. Surprisingly, we did not recapitulate the expected G2/M defect in this line (Figure 7e). We hypothesize that different oncogene activation states or mutations could make it hard to appreciate the difference between GFP and PASD1-GFP cells in H1299 cells. In the cell lines we analyzed, TP53 is inactivated by viral proteins in HEK-293T cells (Abida and Gu, 2003). Furthermore, all of our other lines are TP53 wild type with exception of the H1299, which are homozygous for a *TP53* mutation (Forbes et al. 2014). In human cancer, mutant *TP53* can exert dominant-negative effects over wild type genes and also collaborate with other oncogenes to drive cellular transformation (Olivier et al., 2010). Thus, we hypothesize that mutant *TP53*, or other mutant oncogenes in the cell's genetic background may have led to the unexpected results. Taken together, our cell cycle profiling experiments offer the conclusion that the expression of PASD1 human somatic cells (cancerous and transformed non-cancerous) induces a significant cell cycle defect where cells accumulate at the G2/M transition.

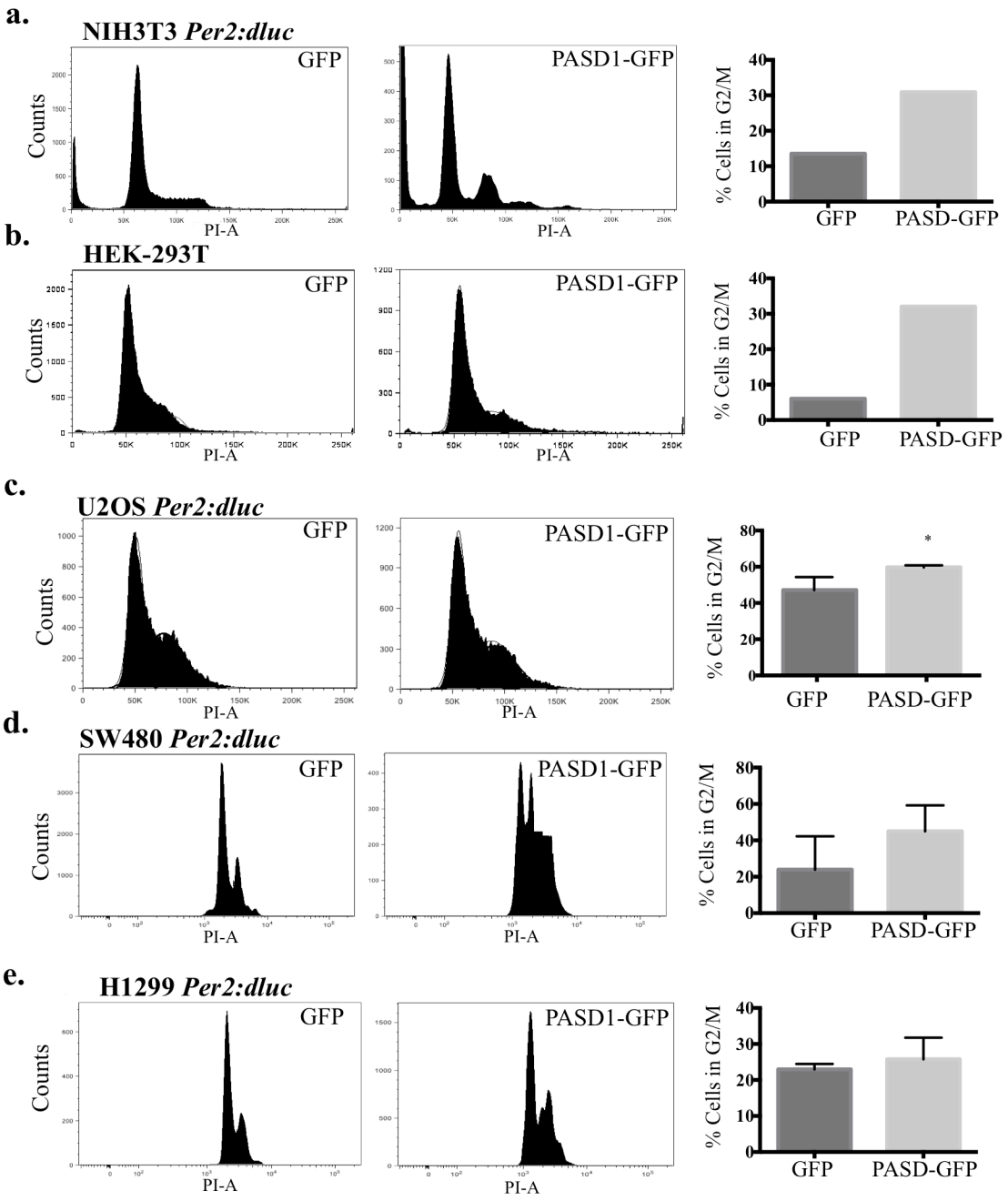

Figure 7. PASD1-GFP Expression in Murine and Human Cell Lines Induces G2/M Arrest. Mouse and human cells that express constitutive GFP and PASD1-GFP were permeabilized with 4% volume / volume (v/v) paraformaldehyde for 15 minutes, fixed with ethanol, and stained with 50 μg/ml propidium iodide to stain DNA. Single cells were excited with a 488 nm laser and analyzed for DNA content using flow cytometry. Cell populations were gated GFP fluorescence and for cells in G2/M cell cycle phase and quantified using FlowJo cell cycle analysis software. The x-axis on the histograms quantifies the area parameter of the voltage read by detector for propidium iodide-positive cells and the y-axis is the number of cells counted at each measured voltage. a.) NIH3T3 *Per2:dluc* n=1, b.) HEK-293T n=1, c.) U2OS *Per2:dluc* n=3, d.) SW480 *Per2:dluc* n=3, e.) H1299 *Per2:dluc* n=2. Values are represented as means ± standard error of mean calculated with GraphPad Prism 6 statistical analysis software. *$p<0.05$.

Overexpression of PASD1 Decreases Cellular Proliferation

Another way to characterize cell cycle profiles and proliferation rate of cells in culture is to use 5-bromo-2′-deoxyuridine (BrdU) labeling. In this method, cell proliferation is measured by quantifying the number of cells undergoing DNA replication by detecting the *de novo* incorporation of thymidine analogs into DNA. This is measured by incubating cultured cells with BrdU for 24 hours, fixing the cells, and then probing with a BrdU primary antibody that is recognized by a horseradish-peroxidase conjugated antibody. To quantify BrdU incorporation, the light absorption of stained cells is read with spectrophotometry. Moreover, the use of BrdU labeling combined with propidium iodide staining of total DNA allows for a clearer distinction between late S phase and G2/M because it separates the populations in a 2D plot, thereby allowing us to infer more about the effects of PASD1 on the proliferative state of cells. We found that U2OS *Per2:dluc* PASD1-GFP expressing cells exhibited a statistically significant (12% ± 8 %) decrease in BrdU incorporation (Figure 8a). These data suggest that PASD1-GFP expression decreases the level of DNA replication and proliferation, which could be a consequence of aberrant mitotic entry.

In our cell cycle analysis of human cancer cells, we noticed that PASD1 did not appear to cause any apoptotic cells as quantifiable by the number of cells that are accumulate in the sub-G_1 area of the cell cycle histogram (Figure 7c-e). These data suggest that cancer cells that express PASD1 are not undergoing increased apoptotic cell death. To unambiguously confirm that decreased proliferation was not due to

increased apoptosis, we next measured apoptotic cell death in PASD1 expressing cancer cells using a more specific assay. To do this, we performed Annexin-V staining and flow cytometry sort to quantify Annexin-V positive cells. In this assay, apoptotic cells with compromised cell membranes allow Annexin-V molecules to bind calcium-dependent phospholipid-binding proteins and phosphatidylserine. Since we collected proliferation data in our U2OS *Per2:dluc* PASD1-GFP and *Per2:dluc* GFP cell pair, we conducted our Annexin-V study in this line. We found that there was no appreciable difference in the number of cells expressing Annexin-V in the cell line pair (Figure 8b). Thus, we can conclude that decreased BrdU incorporation in PASD1-GFP expressing cells was not due to increased levels of apoptosis, but rather decreased cell division.

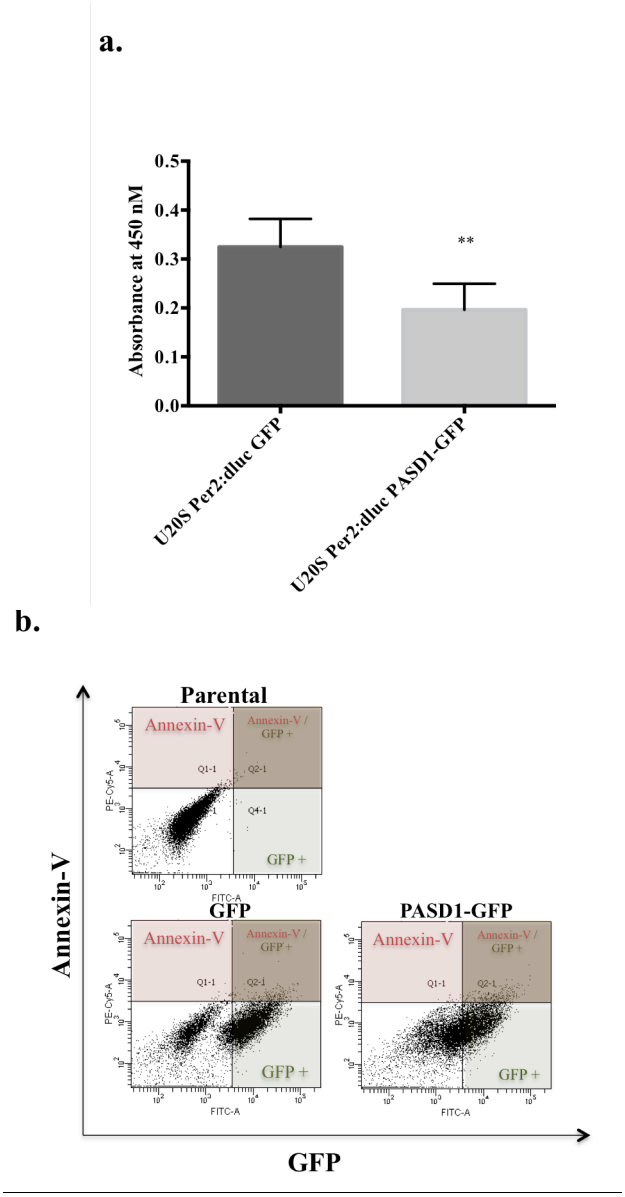

Figure 8. PASD1-GFP Expression in U2OS *Per2:dluc* Cells Slows DNA Synthesis and Does Not Induce Apoptosis

a.) U2OS *Per2:dluc* GFP and U2OS *Per2:dluc* PASD1-GFP cells were cultured in standard conditions and incubated with BrdU thymidine analog for 24 hours in a 48-well flat bottom plate. DNA synthesis was measured by the BrdU incorporation absorbance counts, which is measured by the signal emitted from an ELISA colorimetric assay where absorbance is read at 450 nm. Values are represented as means ± standard error of mean calculated with Graphpad Prism 6 statistical analysis software. n=3, **p<0.01. b.) Representative plots showing single live U2OS *Per2:dluc* GFP and *Per2:dluc* PASD1-GFP cells incubated with Annexin-V molecules conjugated to CY5 fluorophore excited by 649 nm and quantified using flow cytometry and Flowjo analysis software. Quadrants 1 (Q1) and 2(Q2) contain Annexin-V positive, apoptotic populations. n=1.

PASD1 Promotes Aberrant Mitotic Entry and Resistance to Mitotic Spindle Poisoning Drugs

We hypothesize that PASD1-GFP expression results in an increase in mitotic entry and resistance to mitotic spindle poisoning drugs. We subjected U2OS PASD1-GFP cells to cytological profiling using a robotic cell line-screening platform at the University of California Santa Cruz Chemical Screening Center. Use of this platform allows for automated treatment of cell lines with compounds of interest and parallel analysis of the expression levels of mitotic proteins in culture. To do this, the system uses semi-automated antibody probes and signal detection using fluorescence microscopy and computer-aided high throughput image analysis as described in Woehrmann et al. (Woehrmann et al, 2013). We utilized this system to detect and quantify the effects of PASD1-GFP expression and microtubule poisons on mitotic spindle formation in U2OS *Per2:dluc* cells by screening cells for sensitivity to Nocodazole and Paclitaxel. Nocodazole inhibits mitotic spindle microtubule formation by inhibiting the polymerization of microtubules, where Paclitaxel permanently stabilizes microtubules. Both drugs prevent the satisfaction of the Spindle Assembly Checkpoint (SAC) and lead to mitotic spindle collapse and cell death (Jordan and Wilson, 2004; Panvichin et al., 1998).

The expression of other select CT antigens in somatic cancer cells is hypothesized to confer resistance to microtubule poisoning drugs by reinforcing components of the mitotic spindle (Cappell et al, 2012). Based on our previous findings, we

hypothesized that the expression of PASD1-GFP may help to stabilize the mitotic machinery and could confer resistance to the effects of Nocodazole and Paclitaxel treatment. We also hypothesized that PASD1-expressing cells would exhibit a high basal level of mitotic cells and high expression of the components of the mitotic spindle. To test our hypotheses, we employed a stain set that measured DNA content (DAPI), EDU incorporation, anti-phosphorylated Histone 3, and a probe for α–tubulin. EDU staining is analogous to BrdU incorporation where a different thymidine analog is incorporated into DNA, ethnyl-2'-deoxyurdine, and used to measure s-phase cells (Woehrmann et al, 2013). We ran the EDU stain to confirm our BrdU results as an internal control because it was available at the screening center. We probed for Phosphorylated Histone-3 (PH3) because it is specifically phosphorylated in mitosis (Hans and Dimitrov, 2001), and added α-tubulin to our screen because it is cytoskeletal component of microtubules and the mitotic spindle (Kirschner and Mitchinson, 1986).

We began our screen by plating cells in triplicate inside a 24-well plate. Once cells were adherent, we treated experimental wells with a 1% (v/v) dose of Paclitaxel or Nocodazole dissolved in DMSO for 24 hours corresponding to a dose of 500 ng/ml Nocodazole, 100 nM Paclitaxel , or 1 μM Paclitaxel. All of these drug concentrations were used at recommended dosage limits for human cancer cell lines (Brito et al., 2009; Woehrmann et al., 2013; Whitehurst et al., 2007). We also controlled for toxicity caused by DMSO alone by treating a set of control cells were treated with a

1% (v/v) per well of DMSO. After treatment with Nocodazole and Paclitaxel, cells were fixed and stained for DAPI, incubated with EDU for 19 hours, and incubated with primary antibodies to the aforementioned proteins and fluorescent protein conjugated secondary antibodies. EDU incorporation was measured using click chemistry and a FITC conjugated reporter as described Woehrmann et al., 2013. Fluorescence was measured using an automated ImageX- press Micro epifluorescence microscope (Molecular Devices) and images were analyzed using MetaXpress 3.1 software as described in Woehrmann et al., 2013.

Our EDU data recapitulates our BrdU findings to some extent, where PASD1-GFP expression in DMSO treated cells resulted in a more modest 4% decrease in DNA synthesis compared to control GFP cells, as measured by thymidine analog incorporation. Furthermore, the treatment of cells with 500 ng/ml Nocodazole and 100 nM Paclitaxel had little effect on this phenotype, where we report a 5-8% decrease in DNA synthesis in PASD1-GFP cells compared to GFP controls. We did not observe a difference between PASD1-GFP and GFP in cells treated with 1 μM Paclitaxel (Figure 9a). Also, it is important to note that neither Nocodazole nor Paclitaxel caused a decrease in DNA synthesis in GFP or PASD1-GFP cells relative to control. We only observed a difference in EDU incorporation levels when comparing PASD1-GFP to GFP cells. From these data, we conclude that the expression of PASD1-GFP induces a decrease in DNA synthesis, consistent with our earlier BrdU experiments,.

The results of our PH3 foci assay demonstrate that PASD1-GFP expression in DMSO-treated cells induced a 10% increase in the number of mitotic cells when compared to GFP cells, as measured by the ratio of PH3 foci in mitotic to interphase cells as described in Woehrmann et al. 2013 (Figure 9b). Here as well, drug treatment did not change this phenotype, although both doses of Paclitaxel treatment caused a decrease in mitotic cells in GFP cells relative to DMSO control. Interestingly, this was not observed for PASD1-GFP cells, where we observed more cells that entered mitosis than the DMSO-treated GFP or PASD1-GFP control. Thus, from these data it appears that PASD1-GFP-expressing cells were resistant to the reduction in mitotic cells induced by the stabilization of microtubules caused by Paclitaxel (Figure 9b). These data suggest that PASD1-GFP expression increased the number of cells undergoing mitosis and may confer a moderate level of resistance to mitotic spindle poisoning drugs (Figure 9b). These data are also consistent with our finding that PASD1-GFP expression caused on increase in the number of cells that accumulated at the G2/M transition. Taken together, these data argue that PASD1-GFP expression increased the number of cells in in mitosis (Figure 9b).

Next, we investigated the effects of PASD1-GFP expression and drug treatment on α–tubulin density. We found that PASD1-GFP expressing cells treated with DMSO displayed no change in the α–tubulin density per cell compared to their GFP control. However, consistent with Nococazole's mechanism of action, α–tubulin density

decreased by about 50% in both GFP and PASD1-GFP expressing cells after treatment with 500 ug/ml of Nocodazole (Figure 9c). This suggests that Nocodazole inhibited the polymerization of microtubules in both cell lines. Interestingly, we saw no change in α–tubulin density in cells treated with Paclitaxel (Figure 9c).

a.

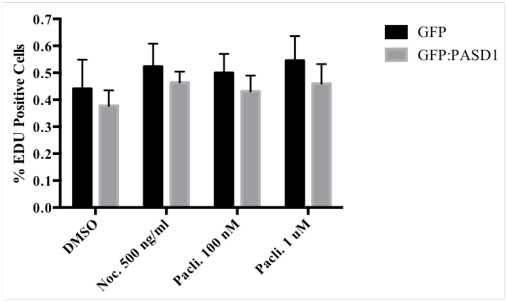

b.

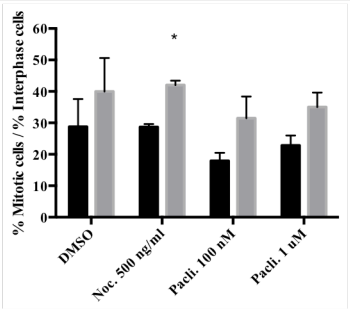

c.

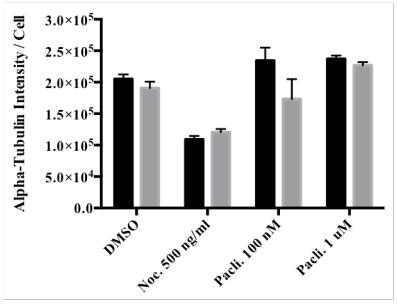

Figure 9. High Content Cytological Screening Profile of U2OS *Per2:dluc* GFP and U2OS *Per2:dluc* PASD1-GFP Expressing Cells

U2OS *Per2:dluc* GFP and U2OS *Per2:dluc* PASD1-GFP cells were plated in triplicate in a 24 well plate. Cells were treated with 1% (v/v) DMSO vehicle control, 500 ng/ml Nocodazole, 100 nM Paclitaxel, and 1 μM Paclitaxel for 24 hours. After treatment, cells were subjected to automated High Content Cytological Screening performed at the UCSC Chemical Screening Center as described in Woehrmann et al. a.) Quantification of the ratio of cells in mitosis to interphase as measured by the quantification of anti-phospho-histone 3 (PH3) staining as described in Woehrmann et al. 2013. b.) Proliferation was measured by EDU incorporation counts, which was detected as described in Woehrmann et al, 2013. c) The quantification of anti-αTubulin density / cell was used to quantify mitotic spindle polymerization. Values are represented as means ± standard error of mean calculated with Graphpad Prism 6 statistical analysis software. n=3, *$p<0.05$.

Human cancer cells silence PASD1 when it is ectopically expressed

Over the course of our studies, we found that U2OS *Per2:dluc* cells silenced PASD1-GFP expression after approximately 6 weeks in culture (Figure 10). This finding was surprising because the use of a lentiviral system with antibiotic selection allowed for stable integration of PASD1-GFP into the genome. Moreover, we did not observe large changes in GFP expression in the control cell line over the same period of time. Thus, we considered the possibility that our cells were selectively silencing PASD1-GFP.

As a strategy to overcome these issues, we decided to make a new stable cell line in our U2OS *Per2:dluc* cells using drug-inducible expression of PASD1-GFP. This strategy appeared to be ideal because it would allow us to induce PASD1-GFP expression shortly before conducting experiments and possibly prevent silencing that might occur due to constitutive overexpression of PASD1-GFP. To do this, we employed the use of a Tet-On-3G two-vector lentiviral expression system (Clontech, USA). In this system, a response vector is used to drive the expression of a gene of interest under the control of a tetracycline-regulated promoter. To activate the expression of the gene of interest, a second regulator vector is used to constitutively express the tetracycline-regulated transgene under the control of the ELFα promoter, which mediates low level expression of the target gene. The tet-transactivator cannot drive the expression of the target gene unless doxycycline is supplied (Shaikh et al., 2006). Thus, with this system we should have been able to drive the expression of

a.

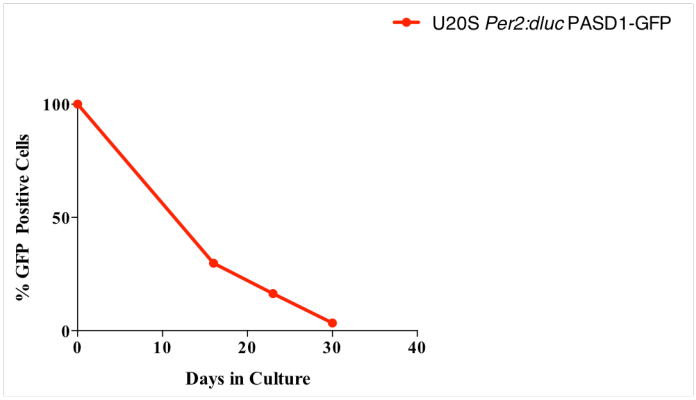

b.

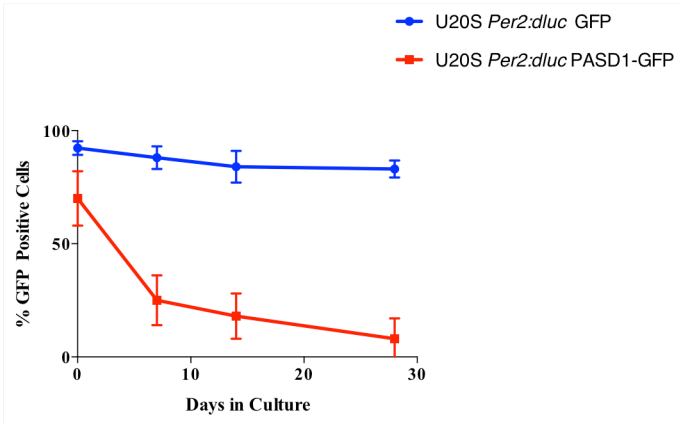

Figure 10. PASD1-GFP Expression Is Silenced After ~30 days in Culture

On the experimental days listed on the x-axis, fluorescence was quantified using fluorescence microscopy and the percent GFP positive cells were quantified using ImageJ analysis software. Data points represent the percentage of GFP positive cells quantified from images photographed at 20X magnification. a.) GFP and PASD1-GFP constitutively expressed in U2OS *Per2:dluc* cells using a lentiviral vector. GFP-positive cells were quantified from one image. b.) GFP or PASD1-GFP were inducibly expressed in U2OS *Per2:dluc* cells using the Tet-on lentiviral vector system. Cells were plated in 6 well plates, and on each induction day, one well of each line was treated with 1 μg/ml doxycycline for 24 hours prior to GFP quantification. GFP-positive cells were quantified and averaged from 10 images.

PASD1-GFP only when we needed it. To introduce the PASD1-GFP or GFP constructs, we simultaneously transduced the tet-regulator vector and the tet-response vector that contains each respective gene of interest in a 1:1 ratio into U2OS *Per2:dluc* cells. After transduction, we then selected clones that successfully integrated the regulator and response vectors. To do this, we selected clones with 1.5 μg/ml Puromycin and 400 μg/ml G418. After selection of stable cell lines, we treated our cells with 1 μg/ml of doxycycline for 24 hours to induce expression of PASD1-GFP or GFP before conducting experiments.

At first, transient expression of PASD1-GFP with doxycycline treatment in U2OS *Per2:dluc* cells seemed to be a solution to our gene silencing issues. To test whether constitutive expression of PASD1-GFP played a role in its progressive silencing, we maintained a primary cell culture in the presence of antibiotics but where expression of PASD1-GFP was never induced. Instead, experimental passages were split off of this 'never-induced' culture for doxycycline induction of PASD1-FDP expression and subsequent experiments. However, despite this careful strategy of maintaining cultures in the absence of PASD1-GFP expression, it became impossible to induce PASD1-GFP expression after roughly 4 weeks in culture (Figure 10). This finding demonstrated to us that ectopic integration of PASD1-GFP into the genomic level was sufficient to control its silencing.

Many human cancer cell lines express endogenous PASD1 (Michael et al., 2015; Uhlen et al., 2015) (Figure 5); thus, it seems plausible that some cell lines that harbor endogenous PASD1 may not silence the gene due to some changes in their genome caused by oncogenic transformation. Therefore, we overexpressed PASD1 and GFP in two cell lines that our lab has characterized to have low basal levels of PASD1 expression (Michael et al., 2015). To do this, we overexpressed PASD1-GFP or GFP with the same CMV driven vector we used in our U2OS *Per2:dluc* experiments. We performed these transductions in H1299 *Per2:dluc* and SW480 *Per2:dluc* cells. These cell lines contained the *Per2:dluc* circadian reporter gene fusions and were previously established by our lab as described in Michael et al. (Liu et al., 2008). Fortunately, this strategy was a success. In both cell lines, PASD1-GFP was not silenced and has held up for months in culture. Successful establishment of stable overexpressing PASD1-GFP H1299 and SW480 cell lines suggests that constitutive overexpression of PASD1-GFP is only stably maintained in cells whose genomes have already been modified in some way to permit expression of this Cancer/Testis antigen.

Full Length PASD1 is found in Micrococcal Nuclease Resistant Insoluble Nuclear Fractions

Our lab is interested in developing assays for the identification of PASD1 binding partners so that we can begin to develop mechanistic hypotheses about how PASD1 functions. To do this, we aim to immunoprecipitate PASD1-GFP and its potential interacting proteins from cells by affinity purification of GFP. We will eventually perform this in PASD1-GFP or GFP expressing SW480 *Per2:dluc* cells because they recapitulate the PASD1-dependent G2/M progression defect. To identify PASD1 interacting proteins, we will use Liquid Chromatography (LC)-Mass Spectrometry (MS)-based methods. To identify and rank order the most relevant peptides in a high-throughput manner, we will utilize a Python module written for our experiment. This script will sort peptides by relevance according to the cell line that they were recovered in, highest spectral counts, and the associated biological gene ontology processes (Figure 11).

PASD1-GFP is exclusively nuclear (Michael et al. 2015)(Figure 6). We know from previous experience that solubilizing PASD1 from whole cell lysates required a brief pulse of low power sonication, using the mechanical force to shear DNA and facilitate the release of PASD1 from chromatin. The ability to retrieve enough soluble PASD1 for immunoprecipitation could be a major hurdle to overcome our study; without soluble PASD1, we will not be able to affinity purify PASD1 or and its binding partners out of cellular lysates. Thus, we set out to optimize a sub-cellular

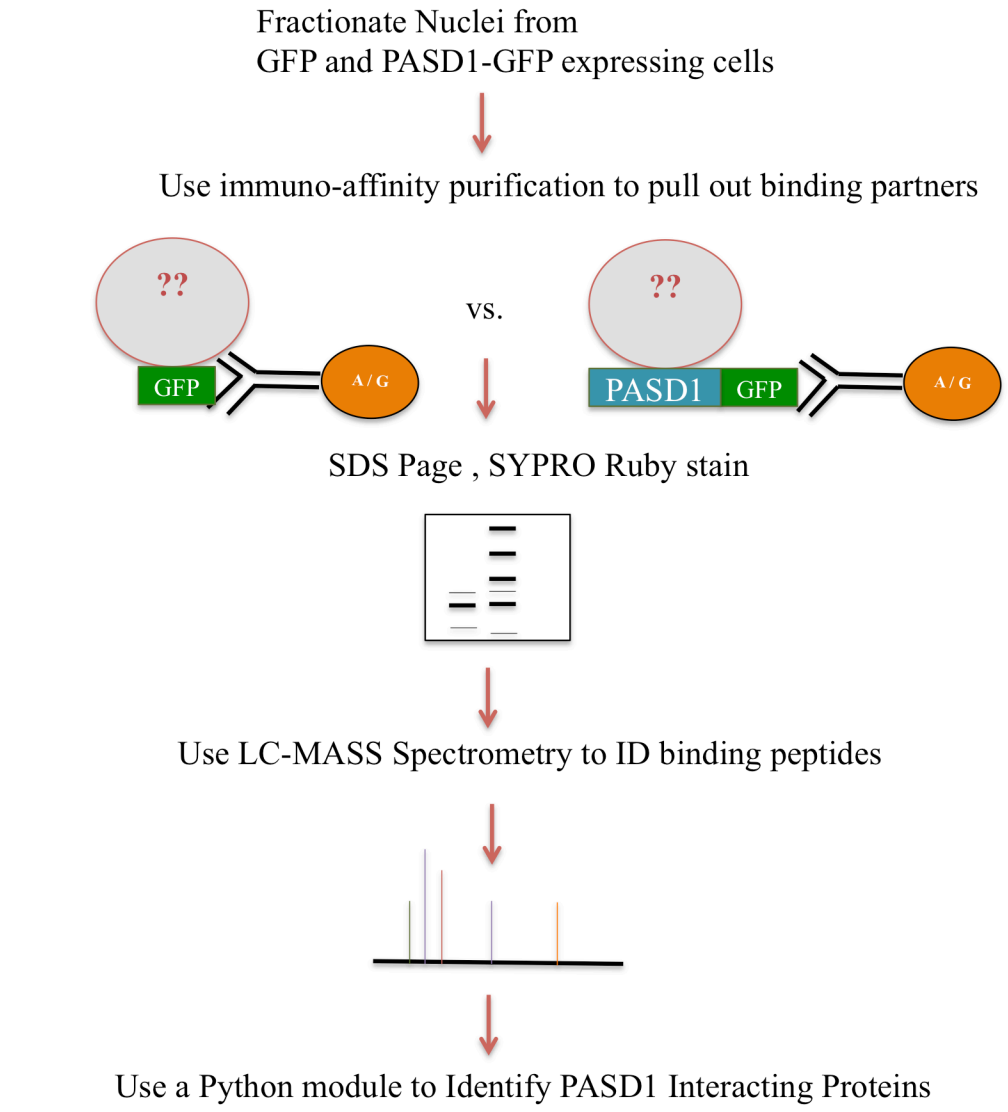

Figure 12. Schematic of Proposed Procedure for Discovery of Novel PASD1 Binding Partners
In future studies, we will fractionate nuclei from isogenic cell line that stably expresses PASD1-GFP or GFP and perform immunoaffinity purification with an anti-GFP antibody to recover proteins. After immunoprecipitation, peptides that bind PASD1-GFP or GFP will be identified with liquid chromatography/mass spectrometry. After peptide identification, we will sort our data with a Python module that finds the most relevant peptides for future study based on spectral counts, nuclear localization, and Gene Ontology Biological Processes.

fractionation assay previously established by our lab that allows us to isolate nuclear components so that we can efficiently scale up the assay to larger cell densities and solubilize enough PASD1 so that we can immunoprecipitate it from lysates.

To perform our assay, we fractionated our cells into insoluble nuclear fractions with a hypotonic lysis buffer before lysing our cells and preforming an immunoprecipitation. We also prepared a lysate not subjected to subcellular fractionation as a control for total PASD1 protein levels. In addition to subcellular fractionation, we also digested cells with micrococcal nuclease. This enhances the solubility of transcriptionally active chromatin by using micrococcal nuclease to digest accessible linker DNA between nucleosomes and digest chromatin into ~150 bp pieces of linker DNA to expose heterochromatin. With this in mind, we set out to fractionate cells down to their insoluble nuclear fraction (containing chromatin) and digest nucleosomes so that we can effectively solubilize PASD1 and free its binding partners from chromatin. To confirm that digestion was efficient, we prepared an additional lysate in our fractionation protocol and extracted DNA using chloroform and ethanol extraction. After extracting DNA, we asked if our digestion resulted in a ladder of fragments ~150 base pairs using agarose gel electrophoresis of our sample.

To express PASD1 for the fractionation experiment, we transiently overexpressed full-length PASD1 with a C-terminal Myc tag in HEK-293T cells . After 48 hours, we fractionated cells down to their insoluble, chromatin containing nuclear fractions

using high-speed centrifugation. To determine what fractions contained chromatin and PASD1-Myc, we subjected all of our isolated fractions to western blot analysis. In our preliminary experiments, we probed for anti-myc and Heterochromatin Protein 1 (HP1). We choose the HP1 probe as a control for nuclear localization and for the presence of chromatin. HP1 protein is found in mostly in heterochromatic regions (Saksouk et al., 2015). The addition of HP1 allows us to further assay the efficiency of micrococcal nuclease digestion and to make hypotheses about whether PASD1 is found in heterochromatin, euchromatin, or if it is present in both regions.

In preliminary studies, we found that PASD1-Myc was only found in micrococcal nuclease-resistant fractions, consistent with localization to heterochromatin regions (Figure 12a). We also found effective conditions for exposing heterochromatin with micrococcal nuclease and were able to visualize ~150 bp pieces of DNA with gel electrophoresis and expose heterochromatin (Figure 12b). The optimization of this fractionation protocol will allow us to scale up the assay and use our H1299 and SW480 cell lines that express constitutive PASD1-GFP. Ultimately, we have optimized a large part of the assay to solubilize PASD1 from chromatin fractions and identify PASD1-interacting proteins. These data will help facilitate future studies on PASD1 interacting proteins.

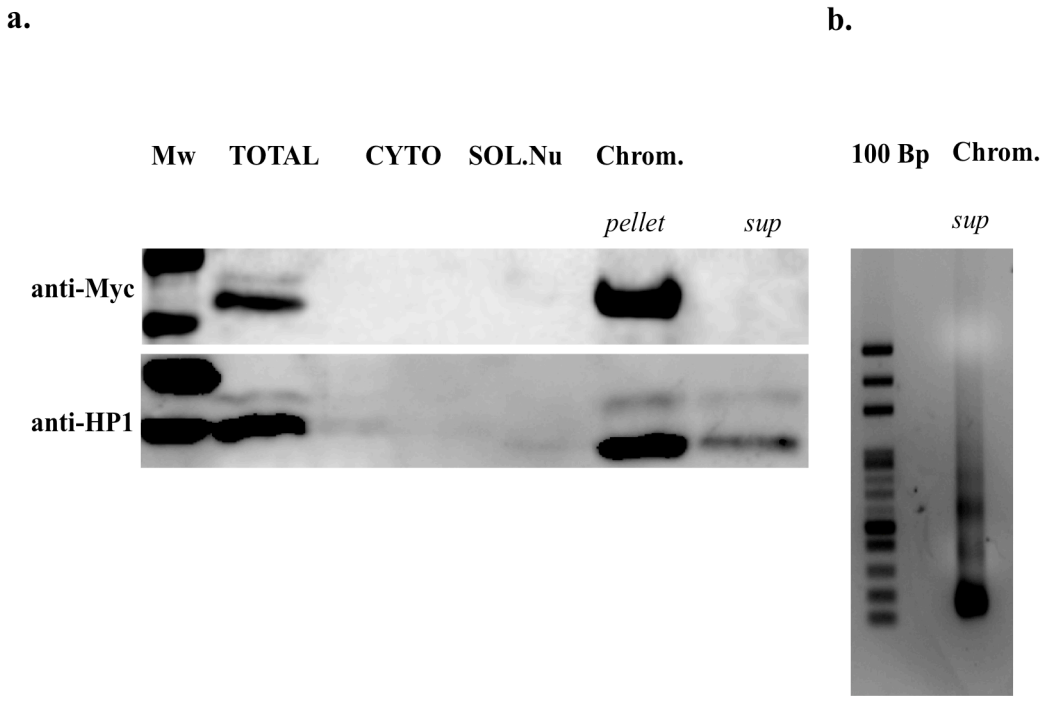

Figure 12. PASD1 is Found in Insoluble Chromatic Cellular Fractions Resistant to Micrococcal Nuclease.
a.) Full-length PASD1-Myc was transiently transfected into HEK-293T cells and cells were lysed 48 hours after transfection. Cell lysates were subjected to subcellular fractionation. Insoluble nuclear fractions were treated with micrococcal nuclease and subjected to high-speed centrifugation to clarify solubilized fragments. Protein samples were prepared and western blot analysis to quantify total Myc and HP1 protein levels was conducted. DNA was extracted from digested chromatin supernatant. Total is a control lysate not subjected to any fractionation, CYTO labels the cytosolic fraction, SOL. Nuc labels the insoluble nuclear fraction, Chrom. labels the nuclear fractions digested with micrococcal nuclease and split into pellet and supernatant. b.) DNA extracted from a chromatin supernatant after 30 minutes of digestion with micrococcal nuclease and high-speed centrifugation.

DISCUSSION

This study establishes that the ectopic expression of PASD1 in human cancer cell lines induces mitotic dysfunction. Specifically, we demonstrate that PASD1 expression promotes abnormal cell cycle progression, where more cells accumulate at the G2/M transition and there is a decrease in the number of cells in S-phase as measured by BrdU incorporation (Figure 7 and Figure 8). Further support for the notion that PASD1 expression induces mitotic dysfunction can be found from our High-Throughput Cytological Profiling experiments, where we found that cells expressing PASD1-GFP have higher levels of mitotic entry as measured by PH3 staining. These data suggest that reactivation of PASD1-GFP expression in somatic cancer cell lines promotes aberrant mitotic entry. Thus, we hypothesize that PASD1 promotes oncogenic transformation of somatic cells. Ultimately, we believe that these defects in cell cycle could be clinically relevant and are worthy of more study.

Often, the accumulation of cells at the G2/M transition is associated with problems of mitotic spindle integrity. Many human cancers have high levels of chromosome mis-segregation and have undergone SAC inactivation or mutation. Over 20 proteins participate in or are associated with the SAC, and many have been linked to tumor progression in humans and mice (Gardener et al., 2000; Bastians et al., 2015; Kapanidou et al., 2015). For example, human gastric cancers frequently show mutations of Mitotic Arrest Deficient 2 (MAD2) and Mitotic checkpoint serine/threonine-protein kinase BUB1 (BUB1). Both of these proteins are

components of the SAC and can lead to aberrant mitotic progression (Kim et al., 2005). Errors in chromosome segregation can lead to chromosome non-disjunction and chromosome loss, which result in aneuploidy. Aneuploidy leads to chromosome instability, which creates a supportive environment for tumor progression (Lengauer et al. 1997). Often, the phenotypes that result from aneuploidy in human cells are quite profound; errors in chromosome segregation resulting in aneuploidy are a hallmark of birth defects, spontaneous abortions, and cancer (Hassold et al., 2001, Thomas et al., 2001).

The finding that PASD1 promotes aberrant mitotic entry could have dire consequences for the somatic cancer cell. For example, overexpression of components of the mitotic spindle could lead mitotic spindle collapse or cause inappropriate attachment of sister chromatids. This phenotype could give rise to aneuploid cells (Gardner and Burke, 2000). In a human cancer, errors in mitotic chromosome segregation that result in aneuploidy, and give rise to genomic instability, which predisposes patients to oncogenic phenotypes. For example, too many chromosomes can cause neoplastic transformation by reducing the dosage of tumor suppressors. Conversely, this can also lead to the amplification of oncogenes (Holy 2002, Hassold et al., 2001).

The promotion of mitotic entry in PASD1 expressing cells could be a consequence of evoking the native germline functions of PASD1. PASD1 is natively expressed in

spermatagonial stem cells that are found in the basement membrane of the seminiferous tubules of the testis that undergo mitosis and subsequent differentiation. These data, taken with the fact that PASD1 potentiates IL-6 cytokine mediated signaling (Xu et al., 2016), suggests that the possibility that PASD1 could use cytokine signaling to evade immune detection in the soma.

One alternative explanation as to why PASD1 expression promotes aberrant mitotic progression is that PASD1 indirectly inhibits cell cycle progression through its inhibition of CLOCK:BMAL1. Most cellular processes are tightly coupled to circadian clock gene expression, where transcripts oscillate in essentially every peripheral tissue to control physiology. Day/night variations in the mitotic index and DNA synthesis occur in many tissues, like the oral mucosa and intestinal epithelium (Panda et al., 2002). It has been established that several genes involved in regulation of mitotic entry, *wee1, cyclinb1,* and *cdc2* are all under circadian control (Cardone and Sassone-Corsi, 2003). The dependence of cell cycle entry on the circadian clock has been demonstrated *in vitro,* as well as *in vivo*. Analysis of circadian cycles in dividing NIH3T3 cells demonstrated that the cell cycle and the circadian clock oscillate in a 1:1 mode-locked state, where cell divisions occurred exactly 5 hours before the peak in circadian *Rev-Erbα* expression (Bieler et al., 2014). *In vivo*, CLOCK:BMAL1 promote the transcription of *Wee1* and control the timing of mitotic entry in regenerating mouse liver (Matsuo et al, 2003). Future studies will be required to ask if PASD1-mediated mitotic defects are a consequence of clock suppression or

an independent phenotype that results from Cancer/Testis antigen activation in somatic cancer cells. Unlike other peripheral tissues, testes do not have a functional circadian clock. In the testes, *Per1* expression is constant over a 24-h period rather than oscillating as it does in tissues with circadian rhythms (Morse et al., 2003). This makes sense because the human testes are one of the most proliferation tissues in the body, where cells undergo extensive mitotic divisions and meiotic divisions throughout life to produce sperm (Cheng et al., 2011).

We show that PASD1 expression is eventually silenced when ectopically expressed in cell lines. When PASD1 is expressed in human cancer cell lines that already exhibit low levels of PASD1 reactivation, its overexpression appears to be tolerated. This suggests there must be a highly significant genomic or epigenetic change that permits the maintenance of PASD1 expression. In future studies, it would be interesting to ask if there is a requirement for the expression of a specific set of genes in order to permit PASD1 expression in somatic cancer cells. To do this, we could use bioinformatics to identify patterns in gene expression unique to human cancer cell lines that endogenously express PASD1.

Conclusion

Our data support the hypothesis that reactivation of PASD1 expression in somatic cells promotes mitotic defects that could favor oncogenic transformation. We show that PASD1-GFP-expressing cells have increased levels of mitotic entry, a decrease

in DNA replication. These phenotypes could promote aneuploidy, which can result in genomic instability and oncogenic transformation. Although the native function of PASD1 is currently unknown, we hypothesize that our observed phenotypes are caused by PASD1 evoking its native functions in somatic cancer cells. Whether the native function of PASD1 is to foster the mitotic divisions in spermatagonial stem cells, suppress the circadian clock in the testis, regulation evasion of immune detection, or something else, remains an open question. Ultimately, this study establishes that PASD1 promotes mitotic defects in somatic cells that may contribute to oncogenic transformation. We also believe that our findings demonstrate the clinical relevance of PASD1 expression in somatic cancer cells. Future studies will be required to mechanistically how PASD1 causes aberrant mitotic progression and to determine if our reported phenotypes are a consequence of clock repression or evoking native PASD1 functions in the somatic cancer cells.

EXPERIMENTAL PROCEDURES

Cell culture

U2OS *Per2:dluc* GFP and U2OS *Per2:dluc* PASD1-GFP cells were established as described in Michael et al., 2015. SW480 and H1299 human cancer cell lines were obtained from ATCC and *Per2:dluc* constructs were stably expressed as described in Michael et al. 2015. After incorporation of the *Per2:dluc* construct, these cells were then transformed with lentiviral constructs to express GFP or PASD1-GFP as previously described in Michael et. al. 2015. Stably transfected clones were selected using empirically determined concentrations of G418 antibiotic that resulted in complete cell death of mock-infected cells. For selection, 800 μg/mL G418 was used to select GFP or PASD1-GFP positive SW480 *Per2:dluc* clones, and 400 μg/ml of G418 for H1299 *Per2:dluc* cell lines. Doxycycline-inducible GFP and PASD1-GFP expressing cells were established with PLVX-ELFα-TET3G lentiviral plasmids as recommended in the Clontech manufacturer's guidelines. All human cancer cell lines used in this work were cultured in their recommended medium: H1299 cells were cultured in RPMI medium (Hyclone, USA) and SW480 and U2OS cell lines were cultured in DMEM medium (Hyclone, USA). All medium was supplemented with 10% (v/v) Fetal Bovine Serum (Fisher scientific, USA) and 1% (v/v) penicillin-streptomycin (Hyclone). All cells were cultured at 37 °C with 5% ambient CO_2.

Generation of Tet-On U2OS *Per2:dluc* Cell Lines

The Tet-On® 3G Inducible Expression System containing pTRE3G and the pELFα-Tet3G vectors were purchased from (Clontech, USA). Full-length PASD1 and GFP were amplified from a pcDNA3B-EGFP vector (Addgene) that we cloned PASD1 into as described in Michael et al. We utilized primers specific to full-length PASD1-GFP designed by Michael et al. After cloning PASD1-GFP into our pTRE3G vector, we packaged both of our vectors using Lenti-X Packaging Single Shots (Clontech, USA) according the manufacturer's protocol. We transduced our packaged vectors simultaneously in a 1:1 ratio in U2OS *Per2:dluc* cells. To select positive clones, we selected cells with 400 μg/ml of G418 and 1.5 μg/ml of puromycin. After selecting clones, we induced expression of PASD1-GFP or GFP by incubating cells with 1 μg/ml of doxycycline. This dose was empirically determined based on manufacturer guidelines.

Transient transfection

Approximately 2 μg of pcDNA3B -PASD1-GFP or pcDNA3B-GFP were used to transfect two 35mm tissue culture-treated petri dishes with 0.3 x 10^6 HEK-293T cells using the lipid-based transfection reagent LT1 (Mirus-bio, USA) as described in Michael et al. 2015. Cells were harvested when peak expression was reached 48 hours after transfection and cells were subjected to FACS analysis.

Analysis of Cell Cycle Progression

Cells were seeded in 25 cm^2 flasks at a density of 0.5 x 10^6 cells / flask. After 24 hours, cells were trypsinized, harvested and fix in 5 ml with 4% (v/v) formaldehyde, and then permeabilized with 100% ice cold ethanol in a volume of 1 ml for 40 minutes. After fixation and permeabilization, cells were pelleted and washed by centrifugation at 1,500 rpm 3X with PBS (137 μM NaCl , 2.7 mM KCL, 10 mM Na^2PO4, 1.8 mM KH^2PO^4). After washing, pellets were suspended in Propidium Iodide (50 μg/ml) staining solution that contained RNase (300 μg / ml) (Cell Signaling Technologies, USA) and stained for 15 minutes on ice as per manufacturer's protocol. After staining, cells were filtered with 53 μm nylon mesh and transferred to flow cytometry compatible assay tubes. The cell cycle distribution of cells based on DNA content stained by propidium iodide was calculated from 100,000 cells using flow cytometry and detection at 488 nm using the BD LSRII flow cytometer (BD Biosciences, USA) and analyzed for cell cycle distributions using Flowjo Single Cell Analysis Software (Flowjo, LLC).

Apoptotic Analysis with Annexin-V Staining

Cells were seeded in 25 cm^2 flasks at a density of 0.5 x 10^6 cells / flask. After 24 hours, cells were washed 3X with cold PBS (0.137 M NaCl, 2.7 mM KCL, 10 mM Na_2PO_4, 1.8 mM KH_2PO_4), and 0.1 x 10^7 cells were resuspended in 1 ml Annexin-V binding buffer (Annexin-V-Cy5 Apoptosis Kit, Biovision, USA). After 15 minutes of incubation on ice, cells were filtered with 53 μm nylon mesh and transferred to flow cytometry-compatible assay tubes. Approximately 5 μl of Annexin-V conjugated to

Cy5 fluorophore was added to each sample and the samples were run on the BD LSRII Flow Cytometer (BD Bioscience, USA) according to the assay kit protocol (Biovision, USA).

High Content Cytological Profiling

U2OS *Per2:dluc* GFP and *Per2:dluc* PASD1-GFP cells were plated in clear bottom 48 well plates (Corning, USA) at an empirically determined density of 0.2 x 10^5 cells per well in Dulbecco's Modified Eagle's Medium (DMEM) (Corning, USA) with 10% FBS. Plates were incubated at 5% ambient CO_2 at 37 °C for 24 hours. Approximately 19 hours after plating, cells were treated with clinically relevant doses of 500 ng/ml Nocodazole or 1 μM Paclitaxel and the plates were incubated at 37 °C and 5% ambient CO_2 for 24 hours. At the 19 hour time point, the plates were transferred to the UCSC Chemical Screening Center for cytological profiling. Fluorescence was measured using an automated ImageX-press Micro epifluorescence microscope (Molecular Devices) and images were analyzed using MetaXpress 3.1 software as described in Woehrmann et al., 2013.

Microscopy

Microscopy of all GFP or PASD1-GFP expressing cells was done using the EVOS XL Digital Inverted Microscope (EVOS, USA). Images were taken using the using phase contrast filter and excitation at 488 nm, where cells emitted 509 nm of light and

light was filtered a 530/20 emission filter. All cells were observed on the 20X objective.

Subcellular Fractionation of Cellular Extracts and Chromatin Digestion

Approximately three 35 mm dishes were plated with 2 ml of 0.15 x 10^5 HEK-293T cells in Dulbecco's Modified Eagles Medium (DMEM, Hyclone, USA) and grown for 24 hours at 37 °C and 5% ambient CO_2. After plating, the cells were transfected using LT-1 lipid-based transfection reagent (Mirus-Bio, USA) with 2 μg of a plasmid containing full-length PASD1, 4B-pcDNA-PASD1-Myc plasmid created in Michael et al. For the total lysate sample, medium was aspirated and cells were incubated on ice for 10 minutes with 200 μl lysis buffer (10 mM HEPES, pH 7.5, 100 mM NaCl, 1mM EDTA), 1% (v/v) Triton X-100, and 5% (v/v) glycerol. The sample was then sonicated using a Sonicator™ Cell Disrupter (Ultrasonics, Inc., USA) with a 1/8" probe. Samples were sonicated on ice at 30% output for 3 3-second pulses. The lysate was clarified at 14,000 rpm at 4°C and 200 μl supernatant was set aside for western blot sample after diluting 6X Sodium Dodecyl Sulfate (SDS) buffer to 1X final concentration.

Cellular fractionation was done by first washing the remaining two 35 mm cell plates with PBS and then scraping cells with 150 μl hypotonic lysis buffer (10 mM HEPES, pH 7.5, 10 mM KCl, 1.5 mM $MgCl_2$, 350 mM Sucrose, 10 % (v/v) Glycerol, 0.1% (v/v) Triton-X-100). Cells were incubated on ice for 10 minutes and then spun down

at 4,000 rpm for 5 minutes at 4 °C. The pellet was saved for isolation of nuclear components of supernatants, and then supernatant were spun down at 14,000 rpm for 2 minutes at 4°C. The cleared supernatant was then transferred to a new tube for western blot analysis as the cytosolic sample. Nuclear lysis was preformed on the resulting nuclear pellet by dispersing the pellet and incubating it with 1% YC lysis buffer on ice for 10 minutes. The soluble nuclear extract was extracted by centrifugation at 14,000 rpm at 4°C and then prepared for western blot analysis with 6X SDS buffer. The insoluble nuclear pellets, the chromatin pellets were saved for digestion with micrococcal nuclease.

To facilitate digestion, the chromatin pellets were resuspended in 150 µl micrococcal nuclease digestion buffer (20 mM HEPES, pH 7.5, 100 mM NaCl, 5mM $CaCl_2$, 0.1% (v/v) Triton-X-100, and 5 % (v/v) Glycerol). Chromatin was digested with 100 units micrococcal nuclease (ThermoFisher Scientific, USA) for 30 minutes at 37 °C. The reaction was stopped with 25 mM EDTA and then the samples were spun down for 5 minutes at 14,000 rpm at 4°C. The supernatants and pellets were then separated; one pellet and one supernatant sample were added to 6X SDS buffer for western blot analysis, while one supernatant was saved for extraction of DNA. To extract DNA, 80 µl of distilled water, 30 µl of SDS, 20 µl of 5M NaCl, and 200 µl of Chloroform were added to the supernatant, vortexed, and spun down at 14,000 rpm for 5 minutes at 4°C. After the first spin, the aqueous phase was removed and put in a new 1.5 ml tube. Next, 1 ml of 100% pure ethanol was added to the tube. The tube was inverted

and then DNA was pelleted at 14,000 rpm for 5 minutes at 4°C. The pellet was rinsed with 75% ethanol and spun down to pellet DNA for 5 minutes. The supernatant was removed and the pellet was carefully air dried. The pellet was suspended in 50 µl TE buffer (10 mM Tris-HCl (pH 8.0) and 0.5 M EDTA) and heated at 55°C until dissolved. For visualization of the digestion ladder, 9 µl of sample was added to 1 µl of 10X SYBER Green nucleic acid stain. The resulting DNA ladder was resolved and visualized on a 2% agarose gel and 100 bp ladder.

Western blotting was done using a 10% polyacrylamide gel and transferred to a nitrocellulose membrane (GE Healthcare, USA). The membrane was blocked in 5% (w/v) low-fat milk in 1X Tris-Buffer Saline with Tween (TBST) (137 mM NaCl, 2.7 mM KCl, 19 mM Tris, 1 ml / liter TWEEN-20 (Sigma-Aldrich, USA) for 1 hour at room temperature, and then incubated with an anti-Myc mouse monoclonal antibody (University of Iowa Developmental Studies Hybridoma Bank, USA, Catalog # 9E10-c) and rabbit anti-HP1 antibodies (ThermoFisher Scientific, USA, Catalog # PA5-17441). To visualize the chemiluminescent signal, the membranes were incubated with IgG-HRP secondary antibodies (Dako, USA) were diluted 1:5,000 (v/v) in 5% low-fat milk/PBS and visualized with Clarity™ Western ECL reagent (GE Healthcare, USA, Catalog # P10026374).

BrdU Cell Proliferation Assay

U2OS *Per2:dluc* cells were seeded in a 48-well flat bottom plate at an empirically determined density of 0.2 x 10^6 cells / well. After 24 hours, cells were treated with 50 μl BrdU (5'-bromo-2'-deoxyuridine) analog and cells were allowed to replicate for 24 hour hours at 5% CO_2 at 37 °C. BrdU incorporation was detected using an ELISA colorimetric assay kit per the manufacturer's protocol (Cell Signaling, USA, Catalog # 6813S).

References

1. Abell AN, Jordan NV, Huang W, et al. MAP3K4/CBP-regulated H2B acetylation controls epithelial-mesenchymal transition in trophoblast stem cells. *Cell Stem Cell*. 2011;8(5):525-537. doi:10.1016/j.stem.2011.03.008.

2. Cappell KM, Sinnott R, Taus P, Maxfield K, Scarbrough M, Whitehurst AW. Multiple cancer testis antigens function to support tumor cell mitotic fidelity. *Mol Cell Biol*. 2012;32(20):4131-4140. doi:10.1128/MCB.00686-12.

3. Jungbluth AA, Ely S, DiLiberto M, et al. The cancer-testis antigens CT7 (MAGE-C1) and MAGE-A3/6 are commonly expressed in multiple myeloma and correlate with plasma-cell proliferation. *Blood*. 2005;106(1):167-174. doi:10.1182/blood-2004-12-4931.

4. Liggins AP, Brown PJ, Asker K, Pulford K, Banham AH. A novel diffuse large B-cell lymphoma-associated cancer testis antigen encoding a PAS domain protein. *Br J Cancer*. 2004;91(1):141-149. doi:10.1038/sj.bjc.6601875.

5. Liggins AP, Lim SH, Soilleux EJ, Pulford K, Banham AH. A panel of cancer-testis genes exhibiting broad-spectrum expression in haematological malignancies. *Cancer Immun*. 2010;10:8. http://www.pubmedcentral.nih.gov/articlerender.fcgi?artid=2964014&tool=pmcentrez&rendertype=abstract. Accessed January 21, 2016.

6. Luo X, Tang Z, Rizo J, Yu H. The Mad2 Spindle Checkpoint Protein Undergoes Similar Major Conformational Changes Upon Binding to Either Mad1 or Cdc20. *Mol Cell*. 2002;9(1):59-71. doi:10.1016/S1097-2765(01)00435-X.

7. Partch CL, Green CB, Takahashi JS. Molecular architecture of the mammalian circadian clock. *Trends Cell Biol*. 2014;24(2):90-99. doi:10.1016/j.tcb.2013.07.002.

8. Sahota SS, Goonewardena CM, Cooper CDO, et al. PASD1 is a potential multiple myeloma-associated antigen. *Blood*. 2006;108(12):3953-3955. doi:10.1182/blood-2006-04-014621.

9. Suzuki H, Ahn HW, Chu T, et al. SOHLH1 and SOHLH2 coordinate spermatogonial differentiation. *Dev Biol*. 2012;361(2):301-312. doi:10.1016/j.ydbio.2011.10.027.

10. Ugarte F, Sousae R, Cinquin B, et al. Progressive Chromatin Condensation and H3K9 Methylation Regulate the Differentiation of Embryonic and Hematopoietic Stem Cells. *Stem cell reports*. 2015;5(5):728-740. doi:10.1016/j.stemcr.2015.09.009.

11. Abida WM, Gu W. p53-Dependent and p53-independent activation of autophagy by ARF. *Cancer Res*. 2008;68(2):352-357. doi:10.1158/0008-5472.CAN-07-2069.

12. Barretina J, Caponigro G, Stransky N, et al. The Cancer Cell Line Encyclopedia enables predictive modelling of anticancer drug sensitivity. *Nature*. 2012;483(7391):603-607. doi:10.1038/nature11003.

13. Bastos RN, Barr FA. Plk1 negatively regulates Cep55 recruitment to the midbody to ensure orderly abscission. *J Cell Biol*. 2010;191(4):751-760. doi:10.1083/jcb.201008108.

14. Bieler J, Cannavo R, Gustafson K, Gobet C, Gatfield D, Naef F. Robust synchronization of coupled circadian and cell cycle oscillators in single mammalian cells. *Mol Syst Biol*. 2014;10:739. http://www.pubmedcentral.nih.gov/articlerender.fcgi?artid=4299496&tool=pmcentrez&rendertype=abstract. Accessed March 4, 2016.

15. Brait M, Sidransky D. Cancer epigenetics: above and beyond. *Toxicol Mech Methods*. 2011;21(4):275-288. doi:10.3109/15376516.2011.562671.

16. Cheng CY, Mruk DD. The blood-testis barrier and its implications for male contraception. *Pharmacol Rev*. 2012;64(1):16-64. doi:10.1124/pr.110.002790.

17. Cheng Y-H, Wong EW, Cheng CY. Cancer/testis (CT) antigens, carcinogenesis and spermatogenesis. *Spermatogenesis*. 2011;1(3):209-220. doi:10.4161/spmg.1.3.17990.

18. Cooper CDO, Lawrie CH, Liggins AP, et al. Identification and characterization of peripheral T-cell lymphoma-associated SEREX antigens. *PLoS One*. 2011;6(8):e23916. doi:10.1371/journal.pone.0023916.

19. Corvinus FM, Orth C, Moriggl R, et al. Persistent STAT3 activation in colon cancer is associated with enhanced cell proliferation and tumor growth. *Neoplasia*. 2005;7(6):545-555. http://www.pubmedcentral.nih.gov/articlerender.fcgi?artid=1501283&tool=pmcentrez&rendertype=abstract. Accessed March 1, 2016.

20. De Smet C, De Backer O, Faraoni I, Lurquin C, Brasseur F, Boon T. The activation of human gene MAGE-1 in tumor cells is correlated with genome-wide

demethylation. *Proc Natl Acad Sci U S A*. 1996;93(14):7149-7153. http://www.pubmedcentral.nih.gov/articlerender.fcgi?artid=38951&tool=pmcentrez&rendertype=abstract. Accessed February 29, 2016.

21. De Smet C, Loriot A, Boon T. Promoter-dependent mechanism leading to selective hypomethylation within the 5' region of gene MAGE-A1 in tumor cells. *Mol Cell Biol*. 2004;24(11):4781-4790. doi:10.1128/MCB.24.11.4781-4790.2004.

22. Delaval B, Doxsey SJ. Pericentrin in cellular function and disease. *J Cell Biol*. 2010;188(2):181-190. doi:10.1083/jcb.200908114.

23. Doyle JM, Gao J, Wang J, Yang M, Potts PR. MAGE-RING protein complexes comprise a family of E3 ubiquitin ligases. *Mol Cell*. 2010;39(6):963-974. doi:10.1016/j.molcel.2010.08.029.

24. Gao J, Aksoy BA, Dogrusoz U, et al. Integrative analysis of complex cancer genomics and clinical profiles using the cBioPortal. *Sci Signal*. 2013;6(269):pl1. doi:10.1126/scisignal.2004088.

25. Heinrich PC, Behrmann I, Haan S, Hermanns HM, Müller-Newen G, Schaper F. Principles of interleukin (IL)-6-type cytokine signalling and its regulation. *Biochem J*. 2003;374(Pt 1):1-20. doi:10.1042/BJ20030407.

26. Honda T, Tamura G, Waki T, et al. Demethylation of MAGE promoters during gastric cancer progression. *Br J Cancer*. 2004;90(4):838-843. doi:10.1038/sj.bjc.6601600.

27. Jungbluth AA, Stockert E, Chen YT, et al. Monoclonal antibody MA454 reveals a heterogeneous expression pattern of MAGE-1 antigen in formalin-fixed

paraffin embedded lung tumours. *Br J Cancer*. 2000;83(4):493-497. doi:10.1054/bjoc.2000.1291.

28. Kalashnikova E V, Revenko AS, Gemo AT, et al. ANCCA/ATAD2 overexpression identifies breast cancer patients with poor prognosis, acting to drive proliferation and survival of triple-negative cells through control of B-Myb and EZH2. *Cancer Res*. 2010;70(22):9402-9412. doi:10.1158/0008-5472.CAN-10-1199.

29. King DP, Zhao Y, Sangoram AM, et al. Positional cloning of the mouse circadian clock gene. *Cell*. 1997;89(4):641-653. http://www.pubmedcentral.nih.gov/articlerender.fcgi?artid=3815553&tool=pmcentrez&rendertype=abstract. Accessed March 1, 2016.

30. KIRSCHNER M. Beyond self-assembly: From microtubules to morphogenesis. *Cell*. 1986;45(3):329-342. doi:10.1016/0092-8674(86)90318-1.

31. Knuth A, Danowski B, Oettgen HF, Old LJ. T-cell-mediated cytotoxicity against autologous malignant melanoma: analysis with interleukin 2-dependent T-cell cultures. *Proc Natl Acad Sci U S A*. 1984;81(11):3511-3515. http://www.pubmedcentral.nih.gov/articlerender.fcgi?artid=345538&tool=pmcentrez&rendertype=abstract. Accessed January 29, 2016.

32. Liu AC, Tran HG, Zhang EE, Priest AA, Welsh DK, Kay SA. Redundant function of REV-ERBalpha and beta and non-essential role for Bmal1 cycling in transcriptional regulation of intracellular circadian rhythms. *PLoS Genet*. 2008;4(2):e1000023. doi:10.1371/journal.pgen.1000023.

33. Meinhardt A, Hedger MP. Immunological, paracrine and endocrine aspects of testicular immune privilege. *Mol Cell Endocrinol*. 2011;335(1):60-68. doi:10.1016/j.mce.2010.03.022.

34. Mondal G, Ohashi A, Yang L, Rowley M, Couch FJ. Tex14, a Plk1-regulated protein, is required for kinetochore-microtubule attachment and regulation of the spindle assembly checkpoint. *Mol Cell*. 2012;45(5):680-695. doi:10.1016/j.molcel.2012.01.013.

35. Mueller JL, Skaletsky H, Brown LG, et al. Independent specialization of the human and mouse X chromosomes for the male germ line. *Nat Genet*. 2013;45(9):1083-1087. doi:10.1038/ng.2705.

36. Nelson PT, Zhang PJ, Spagnoli GC, et al. Cancer/testis (CT) antigens are expressed in fetal ovary. *Cancer Immun*. 2007;7:1. http://www.pubmedcentral.nih.gov/articlerender.fcgi?artid=3077293&tool=pmcentrez&rendertype=abstract. Accessed January 29, 2016.

37. Ohta S, Hamada M, Sato N, Toramoto I. Polyglutamylated Tubulin Binding Protein C1orf96/CSAP Is Involved in Microtubule Stabilization in Mitotic Spindles. *PLoS One*. 2015;10(11):e0142798. doi:10.1371/journal.pone.0142798.

38. Old LJ, Chen YT. New paths in human cancer serology. *J Exp Med*. 1998;187(8):1163-1167. http://www.pubmedcentral.nih.gov/articlerender.fcgi?artid=2212229&tool=pmcentrez&rendertype=abstract. Accessed November 26, 2015.

39. Olivier M, Hollstein M, Hainaut P. TP53 mutations in human cancers: origins, consequences, and clinical use. *Cold Spring Harb Perspect Biol*. 2010;2(1):a001008. doi:10.1101/cshperspect.a001008.

40. Padeken J, Heun P. Nucleolus and nuclear periphery: velcro for heterochromatin. *Curr Opin Cell Biol*. 2014;28:54-60. doi:10.1016/j.ceb.2014.03.001.

41. Panda S, Antoch MP, Miller BH, et al. Coordinated Transcription of Key Pathways in the Mouse by the Circadian Clock. *Cell*. 2002;109(3):307-320. doi:10.1016/S0092-8674(02)00722-5.

42. Saksouk N, Simboeck E, Déjardin J. Constitutive heterochromatin formation and transcription in mammals. *Epigenetics Chromatin*. 2015;8:3. doi:10.1186/1756-8935-8-3.

43. Shaikh S, Nicholson LFB. Optimization of the Tet-On system for inducible expression of RAGE. *J Biomol Tech*. 2006;17(4):283-292. http://www.pubmedcentral.nih.gov/articlerender.fcgi?artid=2291795&tool=pmcentrez&rendertype=abstract. Accessed March 3, 2016.

44. Voutsadakis IA. The network of pluripotency, epithelial-mesenchymal transition, and prognosis of breast cancer. *Breast cancer (Dove Med Press*. 2015;7:303-319. doi:10.2147/BCTT.S71163.

45. White AE, Hieb AR, Luger K. A quantitative investigation of linker histone interactions with nucleosomes and chromatin. *Sci Rep*. 2016;6:19122. doi:10.1038/srep19122.

46. Whitehurst AW, Xie Y, Purinton SC, et al. Tumor antigen acrosin binding protein normalizes mitotic spindle function to promote cancer cell proliferation. *Cancer Res*. 2010;70(19):7652-7661. doi:10.1158/0008-5472.CAN-10-0840.

47. Zhang R, Lahens NF, Ballance HI, Hughes ME, Hogenesch JB. A circadian gene expression atlas in mammals: implications for biology and medicine. *Proc Natl Acad Sci U S A*. 2014;111(45):16219-16224. doi:10.1073/pnas.1408886111.

48. Acevedo HF, Tong JY, Hartsock RJ. Human chorionic gonadotropin-beta subunit gene expression in cultured human fetal and cancer cells of different types and origins. *Cancer*. 1995;76(8):1467-1475. doi:10.1002/1097-0142(19951015)76:8<1467::AID-CNCR2820760826>3.0.CO;2-A.

49. Ait-Tahar K, Liggins AP, Collins GP, et al. Cytolytic T-cell response to the PASD1 cancer testis antigen in patients with diffuse large B-cell lymphoma. *Br J Haematol*. 2009;146(4):396-407. doi:10.1111/j.1365-2141.2009.07761.x.

50. Bastians H. Causes of Chromosomal Instability. *Recent results cancer Res Fortschritte der Krebsforsch Progrès dans les Rech sur le cancer*. 2015;200:95-113. doi:10.1007/978-3-319-20291-4_5.

51. Bettoni F, Filho FC, Grosso DM, et al. Identification of FAM46D as a novel cancer/testis antigen using EST data and serological analysis. *Genomics*. 2009;94(3):153-160. doi:10.1016/j.ygeno.2009.06.001.

52. Busino L, Bassermann F, Maiolica A, et al. SCFFbxl3 controls the oscillation of the circadian clock by directing the degradation of cryptochrome proteins. *Science*. 2007;316(5826):900-904. doi:10.1126/science.1141194.

53. Cardone L, Sassone-Corsi P. Timing the cell cycle. *Nat Cell Biol*. 2003;5(10):859-861. doi:10.1038/ncb1003-859.

54. Ciró M, Prosperini E, Quarto M, et al. ATAD2 is a novel cofactor for MYC, overexpressed and amplified in aggressive tumors. *Cancer Res*. 2009;69(21):8491-8498. doi:10.1158/0008-5472.CAN-09-2131.

55. Cooper CDO, Liggins AP, Ait-Tahar K, Roncador G, Banham AH, Pulford K. PASD1, a DLBCL-associated cancer testis antigen and candidate for lymphoma immunotherapy. *Leukemia*. 2006;20(12):2172-2174. doi:10.1038/sj.leu.2404424.

56. Coral S, Sigalotti L, Altomonte M, et al. 5-aza-2'-deoxycytidine-induced expression of functional cancer testis antigens in human renal cell carcinoma: immunotherapeutic implications. *Clin Cancer Res*. 2002;8(8):2690-2695. http://www.ncbi.nlm.nih.gov/pubmed/12171902. Accessed March 12, 2016.

57. Costa FF, Le Blanc K, Brodin B. Concise review: cancer/testis antigens, stem cells, and cancer. *Stem Cells*. 2007;25(3):707-711. doi:10.1634/stemcells.2006-0469.

58. De Smet C, Lurquin C, Lethé B, Martelange V, Boon T. DNA Methylation Is the Primary Silencing Mechanism for a Set of Germ Line- and Tumor-Specific Genes with a CpG-Rich Promoter. *Mol Cell Biol*. 1999;19(11):7327-7335. doi:10.1128/MCB.19.11.7327.

59. Dictenberg JB, Zimmerman W, Sparks CA, et al. Pericentrin and γ-Tubulin Form a Protein Complex and Are Organized into a Novel Lattice at the Centrosome. *J Cell Biol*. 1998;141(1):163-174. doi:10.1083/jcb.141.1.163.

60. Djureinovic D, Fagerberg L, Hallström B, et al. The human testis-specific proteome defined by transcriptomics and antibody-based profiling. *Mol Hum Reprod*. 2014;20(6):476-488. doi:10.1093/molehr/gau018.

61. Forbes SA, Beare D, Gunasekaran P, et al. COSMIC: exploring the world's knowledge of somatic mutations in human cancer. *Nucleic Acids Res*. 2014;43(D1):D805-D811. doi:10.1093/nar/gku1075.

62. Gardner RD, Burke DJ. The spindle checkpoint: two transitions, two pathways. *Trends Cell Biol*. 2000;10(4):154-158. http://www.ncbi.nlm.nih.gov/pubmed/10740270. Accessed February 18, 2016.

63. Gekakis N, Staknis D, Nguyen HB, et al. Role of the CLOCK protein in the mammalian circadian mechanism. *Science*. 1998;280(5369):1564-1569. http://www.ncbi.nlm.nih.gov/pubmed/9616112. Accessed November 19, 2015.

64. Godinho SIH, Maywood ES, Shaw L, et al. The after-hours mutant reveals a role for Fbxl3 in determining mammalian circadian period. *Science*. 2007;316(5826):897-900. doi:10.1126/science.1141138.

65. Gurchot C. The trophoblast theory of cancer (John Beard, 1857-1924) revisited. *Oncology*. 1975;31(5-6):310-333. http://www.ncbi.nlm.nih.gov/pubmed/1107920. Accessed January 26, 2016.

66. Güre AO, Wei IJ, Old LJ, Chen Y-T. The SSX gene family: characterization of 9 complete genes. *Int J cancer*. 2002;101(5):448-453. doi:10.1002/ijc.10634.

67. Han C, Kwon JT, Park I, et al. Impaired sperm aggregation in Adam2 and Adam3 null mice. *Fertil Steril*. 2010;93(8):2754-2756. doi:10.1016/j.fertnstert.2010.03.013.

68. Hans F, Dimitrov S. Histone H3 phosphorylation and cell division. *Oncogene*. 2001;20(24):3021-3027. doi:10.1038/sj.onc.1204326.

69. Hassold T, Hunt P. To err (meiotically) is human: the genesis of human aneuploidy. *Nat Rev Genet*. 2001;2(4):280-291. doi:10.1038/35066065.

70. Holy JM. Curcumin disrupts mitotic spindle structure and induces micronucleation in MCF-7 breast cancer cells. *Mutat Res*. 2002;518(1):71-84. http://www.ncbi.nlm.nih.gov/pubmed/12063069. Accessed February 13, 2016.

71. James SR, Link PA, Karpf AR. Epigenetic regulation of X-linked cancer/germline antigen genes by DNMT1 and DNMT3b. *Oncogene*. 2006;25(52):6975-6985. doi:10.1038/sj.onc.1209678.

72. Jang SJ, Soria J-C, Wang L, et al. Activation of Melanoma Antigen Tumor Antigens Occurs Early in Lung Carcinogenesis. *Cancer Res*. 2001;61(21):7959-7963. http://cancerres.aacrjournals.org/content/61/21/7959.long. Accessed February 23, 2016.

73. Joseph-Pietras D, Gao Y, Zojer N, et al. DNA vaccines to target the cancer testis antigen PASD1 in human multiple myeloma. *Leukemia*. 2010;24(11):1951-1959. doi:10.1038/leu.2010.196.

74. Kapanidou M, Lee S, Bolanos-Garcia VM. BubR1 kinase: protection against aneuploidy and premature aging. *Trends Mol Med*. 2015;21(6):364-372. doi:10.1016/j.molmed.2015.04.003.

75. Kim H-S, Park KH, Kim SA, et al. Frequent mutations of human Mad2, but not Bub1, in gastric cancers cause defective mitotic spindle checkpoint. *Mutat Res*. 2005;578(1-2):187-201. doi:10.1016/j.mrfmmm.2005.05.020.

76. Kimmins S, Sassone-Corsi P. Chromatin remodelling and epigenetic features of germ cells. *Nature*. 2005;434(7033):583-589. doi:10.1038/nature03368.

77. Lengauer C, Kinzler KW, Vogelstein B. Genetic instability in colorectal cancers. *Nature*. 1997;386(6625):623-627. doi:10.1038/386623a0.

78. Loriot A, De Plaen E, Boon T, De Smet C. Transient down-regulation of DNMT1 methyltransferase leads to activation and stable hypomethylation of MAGE-A1 in melanoma cells. *J Biol Chem*. 2006;281(15):10118-10126. doi:10.1074/jbc.M510469200.

79. Louhimo J, Alfthan H, Stenman U-H, Haglund C. Serum HCG beta and CA 72-4 are stronger prognostic factors than CEA, CA 19-9 and CA 242 in pancreatic cancer. *Oncology*. 2004;66(2):126-131. doi:10.1159/000077438.

80. Mannan AU, Nayernia K, Mueller C, Burfeind P, Adham IM, Engel W. Male mice lacking the Theg (testicular haploid expressed gene) protein undergo normal spermatogenesis and are fertile. *Biol Reprod*. 2003;69(3):788-796. doi:10.1095/biolreprod.103.017400.

81. Matsuo T, Yamaguchi S, Mitsui S, Emi A, Shimoda F, Okamura H. Control mechanism of the circadian clock for timing of cell division in vivo. *Science*. 2003;302(5643):255-259. doi:10.1126/science.1086271.

82. Mattout A, Biran A, Meshorer E. Global epigenetic changes during somatic cell reprogramming to iPS cells. *J Mol Cell Biol*. 2011;3(6):341-350. doi:10.1093/jmcb/mjr028.

83. Michael AK, Harvey SL, Sammons PJ, et al. Cancer/Testis Antigen PASD1 Silences the Circadian Clock. *Mol Cell*. 2015. doi:10.1016/j.molcel.2015.03.031.

84. Morse D, Cermakian N, Brancorsini S, Parvinen M, Sassone-Corsi P. No circadian rhythms in testis: Period1 expression is clock independent and developmentally regulated in the mouse. *Mol Endocrinol*. 2003;17(1):141-151. doi:10.1210/me.2002-0184.

85. Nicholson RI, Gee JM, Harper ME. EGFR and cancer prognosis. *Eur J Cancer*. 2001;37 Suppl 4:S9-S15. http://www.ncbi.nlm.nih.gov/pubmed/11597399. Accessed February 29, 2016.

86. Nishimoto N, Kishimoto T. Interleukin 6: from bench to bedside. *Nat Clin Pract Rheumatol*. 2006;2(11):619-626. doi:10.1038/ncprheum0338.

87. Pineda CT, Potts PR. Oncogenic MAGEA-TRIM28 ubiquitin ligase downregulates autophagy by ubiquitinating and degrading AMPK in cancer. *Autophagy*. 2015;11(5):844-846. doi:10.1080/15548627.2015.1034420.

88. Pineda CT, Ramanathan S, Fon Tacer K, et al. Degradation of AMPK by a cancer-specific ubiquitin ligase. *Cell*. 2015;160(4):715-728. doi:10.1016/j.cell.2015.01.034.

89. Preitner N, Damiola F, Lopez-Molina L, et al. The orphan nuclear receptor REV-ERBalpha controls circadian transcription within the positive limb of the mammalian circadian oscillator. *Cell*. 2002;110(2):251-260. http://www.ncbi.nlm.nih.gov/pubmed/12150932. Accessed February 27, 2016.

90. Rato L, Alves MG, Socorro S, Duarte AI, Cavaco JE, Oliveira PF. Metabolic regulation is important for spermatogenesis. *Nat Rev Urol*. 2012;9(6):330-338. doi:10.1038/nrurol.2012.77.

91. Sato TK, Panda S, Miraglia LJ, et al. A functional genomics strategy reveals Rora as a component of the mammalian circadian clock. *Neuron*. 2004;43(4):527-537. doi:10.1016/j.neuron.2004.07.018.

92. Scanlan MJ, Gure AO, Jungbluth AA, Old LJ, Chen Y-T. Cancer/testis antigens: an expanding family of targets for cancer immunotherapy. *Immunol Rev*. 2002;188:22-32. http://www.ncbi.nlm.nih.gov/pubmed/12445278. Accessed December 1, 2015.

93. Simpson AJG, Caballero OL, Jungbluth A, Chen Y-T, Old LJ. Cancer/testis antigens, gametogenesis and cancer. *Nat Rev Cancer*. 2005;5(8):615-625. doi:10.1038/nrc1669.

94. Sugita M, Geraci M, Gao B, et al. Combined use of oligonucleotide and tissue microarrays identifies cancer/testis antigens as biomarkers in lung carcinoma. *Cancer*

Res. 2002;62(14):3971-3979. http://www.ncbi.nlm.nih.gov/pubmed/12124329. Accessed January 29, 2016.

95. Thomas NS, Ennis S, Sharp AJ, et al. Maternal sex chromosome non-disjunction: evidence for X chromosome-specific risk factors. *Hum Mol Genet*. 2001;10(3):243-250. http://www.ncbi.nlm.nih.gov/pubmed/11159943. Accessed February 18, 2016.

96. Uhlen M, Fagerberg L, Hallstrom BM, et al. Tissue-based map of the human proteome. *Science (80-)*. 2015;347(6220):1260419-1260419. doi:10.1126/science.1260419.

97. Ukai-Tadenuma M, Yamada RG, Xu H, Ripperger JA, Liu AC, Ueda HR. Delay in feedback repression by cryptochrome 1 is required for circadian clock function. *Cell*. 2011;144(2):268-281. doi:10.1016/j.cell.2010.12.019.

98. van der Bruggen P, Traversari C, Chomez P, et al. A gene encoding an antigen recognized by cytolytic T lymphocytes on a human melanoma. *Science*. 1991;254(5038):1643-1647. http://www.ncbi.nlm.nih.gov/pubmed/1840703. Accessed December 2, 2015.

99. Van Pel A, van der Bruggen P, Coulie PG, et al. Genes coding for tumor antigens recognized by cytolytic T lymphocytes. *Immunol Rev*. 1995;145:229-250. http://www.ncbi.nlm.nih.gov/pubmed/7590828. Accessed January 26, 2016.

100. Watson RE, Curtin GM, Doolittle DJ, Goodman JI. Progressive alterations in global and GC-rich DNA methylation during tumorigenesis. *Toxicol Sci*. 2003;75(2):289-299. doi:10.1093/toxsci/kfg190.

101. Weber J, Salgaller M, Samid D, et al. Expression of the MAGE-1 tumor antigen is up-regulated by the demethylating agent 5-aza-2'-deoxycytidine. *Cancer Res*. 1994;54(7):1766-1771. http://www.ncbi.nlm.nih.gov/pubmed/7511051. Accessed March 12, 2016.

102. Weber J, Salgaller M, Samid D, et al. Expression of the MAGE-1 Tumor Antigen Is Up-Regulated by the Demethylating Agent 5-Aza-2'-Deoxycytidine. *Cancer Res*. 1994;54(7):1766-1771. http://cancerres.aacrjournals.org/content/54/7/1766.abstract. Accessed March 12, 2016.

103. Whitehurst AW. Cause and consequence of cancer/testis antigen activation in cancer. *Annu Rev Pharmacol Toxicol*. 2014;54(1):251-272. doi:10.1146/annurev-pharmtox-011112-140326.

104. Whitehurst AW, Bodemann BO, Cardenas J, et al. Synthetic lethal screen identification of chemosensitizer loci in cancer cells. *Nature*. 2007;446(7137):815-819. doi:10.1038/nature05697.

105. Woehrmann MH, Bray WM, Durbin JK, et al. Large-scale cytological profiling for functional analysis of bioactive compounds. *Mol Biosyst*. 2013;9(11):2604-2617. doi:10.1039/c3mb70245f.

106. Xu Z-S, Zhang H-X, Zhang Y-L, et al. PASD1 promotes STAT3 activity and tumor growth by inhibiting TC45-mediated dephosphorylation of STAT3 in the nucleus. *J Mol Cell Biol*. 2016. doi:10.1093/jmcb/mjw005.